



Unraveling dynamic protein structures by two-dimensional infrared spectra with a pretrained machine learning model

Fan Wu^{a,1}, Yan Huang^{a,1}, Guokun Yang^{a,1}, Sheng Ye^{b,2}, Shaul Mukamel^{c,2}, and Jun Jiang^{a,2}

Contributed by Shaul Mukamel; received May 9, 2024; accepted May 28, 2024; reviewed by Gregory D. Scholes and Martin T. Zanni

Dynamic protein structures are crucial for deciphering their diverse biological functions. Two-dimensional infrared (2DIR) spectroscopy stands as an ideal tool for tracing rapid conformational evolutions in proteins. However, linking spectral characteristics to dynamic structures poses a formidable challenge. Here, we present a pretrained machine learning model based on 2DIR spectra analysis. This model has learned signal features from approximately 204,300 spectra to establish a "spectrum-structure" correlation, thereby tracing the dynamic conformations of proteins. It excels in accurately predicting the dynamic content changes of various secondary structures and demonstrates universal transferability on real folding trajectories spanning timescales from microseconds to milliseconds. Beyond exceptional predictive performance, the model offers attention-based spectral explanations of dynamic conformational changes. Our 2DIR-based pretrained model is anticipated to provide unique insights into the dynamic structural information of proteins in their native environments.

ultrafast spectroscopy | protein dynamics | machine learning

Protein structures are pivotal for elucidating their diverse biological functions. Significant experimental advancements have been made in the determination of protein structure (1-3). In recent years, AI has shown promising success in determining the lowest-energy state of proteins (4-18). Tools like AlphaFold2 (4, 5) and RoseTTAFold (6) can predict the three-dimensional structures of proteins from their amino acid sequences, while the integration of message passing neural network (MPNN) supplements the predictive capability of protein assemblies (8). The latest generative models can sample a broad variety of protein structures based on desired properties (13-16). These advancements have deepened our understanding of the lowest-energy static protein structures. Given that the dynamic characteristics of proteins ultimately shape their biological functions (19), integrating conformational dynamics information into machine learning (ML) training is therefore crucial for identifying dynamic protein structures that are relevant to biological processes (20-22).

Optical signals offer a unique window into protein dynamic responses. Two-dimensional infrared (2DIR) spectroscopy, based on femtosecond pulse sequences, has proven to be a powerful tool for determining protein structure and provides snapshots of protein folding events (23-30). However, unraveling dynamic protein structures from a series of 2DIR spectra present a formidable task, which typically requires days or weeks of manual analysis by a trained expert. Recent efforts in applying ML methods to extract structural information from spectroscopic signals (31–35) have paved the way for the potential of tracing protein dynamics. Therefore, it is imperative to develop data-driven ML protocols for automatically establishing correlations between protein 2DIR spectra and their dynamic conformations.

Here, we introduce a ML pretrained model utilizing the state-of-the-art transformer architecture (36), which effectively learns the signal features from 2DIR spectra and establishes a 'spectrum-structure" correlation, thereby enabling the prediction of dynamic contents of various secondary structures in proteins. After being pretrained on approximately 204,300 simulated 2DIR spectra, the model shows exceptional transferability to real protein folding trajectories covering timescales from microseconds to milliseconds. Beyond its universal predictive power, this model also allows one to obtain signal interpretation for structure identification from the original spectra through attention maps. By tracing conformational changes in protein dynamics via 2DIR spectroscopy, this model can provide critical insights into the dynamic behavior of proteins and their biological function.

Results

Overall Schematic and ML Model Architecture. Our experimental workflow, illustrated in Fig. 1A, encompasses "construction of the 2DIR spectra dataset," "pretraining of the

Significance

Unraveling dynamic protein structures from two-dimensional infrared (2DIR) spectral signals presents a formidable task. By utilizing machine learning, we have correlated the intricate 2DIR spectroscopic features with the protein dynamic conformations, thereby tracing changes of secondary structure content along protein folding trajectories. This pretrained model facilitates universal transfer learning across diverse protein folding trajectories, offering valuable insights into the dynamic behavior of proteins and their biological function.

Author affiliations: aKey Laboratory of Precision and Intelligent Chemistry, Hefei National Research Center for Physical Sciences at the Microscale, School of Chemistry and Materials Science, University of Science and Technology of China, Hefei 230026, Anhui, China; ^bAnhui Provincial Engineering Research Center for Unmanned System and Intelligent Technology, School of Artificial Intelligence, Anhui University, Hefei 230601, Anhui, China; and ^cDepartment of Chemistry and of Physics & Astronomy, University of California, Irvine, CA 92697

Author contributions: F.W., S.Y., S.M., and J.J. designed research; F.W., Y.H., and G.Y. performed research; F.W., Y.H., and G.Y. contributed new reagents/analytic tools; F.W., Y.H., G.Y., S.Y., S.M., and J.J. analyzed data; and F.W., Y.H., G.Y., S.Y., S.M., and J.J. wrote the paper.

Reviewers: G.D.S., Princeton University; and M.T.Z., University of Wisconsin-Madison.

The authors declare no competing interest.

Copyright © 2024 the Author(s). Published by PNAS. This article is distributed under Creative Commons Attribution-NonCommercial-NoDerivatives License 4.0 (CC BY-NC-ND).

¹F.W., Y.H., and G.Y. contributed equally to this work.

²To whom correspondence may be addressed. Email: yess@mail.ustc.edu.cn, smukamel@uci.edu, or jiangj1@ ustc.edu.cn.

This article contains supporting information online at https://www.pnas.org/lookup/suppl/doi:10.1073/pnas. 2409257121/-/DCSupplemental.

Published June 25, 2024.

model," and "transfer learning to protein folding trajectories," all structured in a straightforward hierarchy. The 2DIR spectra pretraining dataset is generated by simulations, with detailed steps shown in Fig. 1B. We extracted 4,086 distinct homologous superfamily protein structures from the Orengo et al. developed CATH database, version 4.3 (37). The complete file index used in this study is available in SI Appendix. To capture dynamic information, 50 snapshots were taken for each trajectory at 1-ns intervals following molecular dynamics (MD) equilibrium, yielding a total of 204,300 protein conformations. The Hamiltonians for each protein conformation within the amide I spectral window were derived using semiempirical vibrational spectroscopic maps (38, 39), and the 2DIR signals were simulated employing the NISE code developed by Jansen et al. (40, 41). The contents of different secondary structures, including helix, strand, and coil were determined by utilizing the Stride program (42). The combined 2DIR spectra and secondary structure content formed the pretraining dataset.

The detailed architecture of our model is shown in Fig. 1*C*, based on the Vision Transformer (36). The 2DIR signals used for learning span the 1,575 to 1,725 cm⁻¹ spectral window, where the horizontal and vertical axes correspond to coherence and detection frequency, respectively. Each spectrum is converted into a 224×224 matrix, segmented into 16×16 small patches, and subsequently flattened for model input. The position embeddings and an extra learnable regression [RGS] token to estimate the secondary

structure contents were incorporated. The Transformer Encoder is composed of 12 alternating sets of multiheaded self-attention (MSA) layers and multilayer perceptron (MLP) layers, with pre-layernorm (LN) technique (43, 44) being utilized. The [RGS] token, as the output from the Transformer Encoder, is assumed to capture the essential spectral features of the 2DIR signal. It then proceeds through a MLP layer to predict the secondary structure contents of protein conformations.

The notable advantage of the pretrained model lies in its capability to show good predictive performance on entirely new, unseen datasets. In *Transfer Learning* at the bottom of Fig. 1*A*, the proficiency of our model in predicting the dynamic secondary structure contents during the reversible folding processes of Trp-cage and WW domain proteins serves as an illustrative example. The transferability to the folding trajectories of $\alpha 3D$ and ubiquitin proteins will be demonstrated in the following. Additionally, the attention weights from the MSA layer can be extracted for visualization, showcasing which regions of the 2DIR spectra are most significant when predicting the contents of various secondary structures.

Pretraining Results on the CATH Dataset. The pretraining task is pivotal for determining the performance of the ensuing transfer learning process. During this phase, the model has to be trained on a vast and varied dataset to assimilate the intricate signal patterns and features of 2DIR spectra. Within our spectral dataset of 204,300 entries, 20% was allocated as a validation set, and 50 to

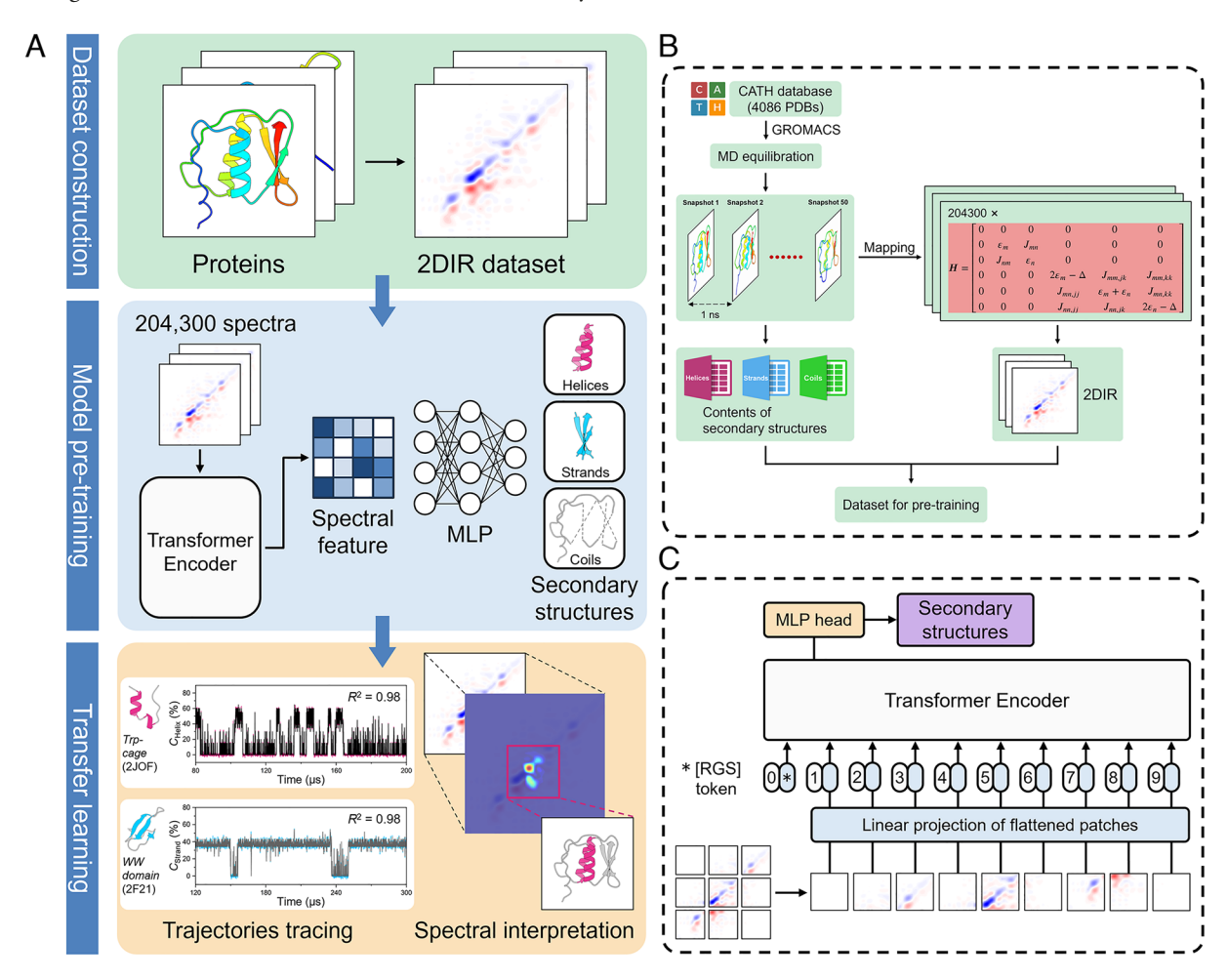


Fig. 1. Comprehensive workflow to predict dynamic protein secondary structures. (*A*) The overall experimental sequence flows from top to bottom, encompassing construction of the 2DIR spectra dataset, pretraining of the model, and transfer learning to protein folding trajectories. The C_{Helix} of Trp-cage and the C_{Strand} of WV domain respectively represent the contents of helices and strands within the overall secondary structure, expressed as a percentage. (*B*) For the pretraining dataset, protein entries underwent MD equilibration before each snapshot was taken to simulate 2DIR spectra and quantify secondary structure contents. (*C*) Detailed architecture of the ML model.

80% was employed as a training set to determine the minimum data amount required. Our findings suggest that utilizing at least 75% of the training set is necessary to achieve satisfactory prediction results, with a coefficient of determination (R^2) of 0.98 and a root mean squared error (RMSE) of 1.87 (SI Appendix, Fig. S1). The model has the capacity to concurrently predict the contents of three secondary structures for a single protein conformation. The error distribution of the validation set depicted in *SI Appendix*, Fig. S2 shows that the mean absolute error (MAE) for 96.54% of the predictions falls below 3.00. C_{Helix} , C_{Strand} , and C_{Coil} are represented as the content of the corresponding secondary structures, namely helix, strand, and coil. When examining the specific predictive contents for each secondary structure, as illustrated in the scatter plot of Fig. 2A, the R^2 value of helix, strand, and coil are 0.99, 0.98, and 0.98, respectively. Meanwhile, their RMSE are 1.51%,1.89%, and 1.71%, respectively, demonstrating the robust regression performance of the model.

To investigate the ability of the model to predict the dynamic content changes of secondary structures, we selected a total of 30 entries based on the protein molecular weight distribution in the CATH database. A 100-ns MD simulation was then performed, extending the initial 50-ns trajectory. The changes in secondary structure content over time were counted and the 2DIR spectra were calculated. As shown in *SI Appendix*, Fig. S3, the three major structural classes of proteins (mainly helix, mainly strand, and mixed helix/strand) in the database mostly contain about 20 to 200 amino acid residues. Thus, taking the mainly helix class as an example, for proteins with ≤200 amino acid residues, we began with a 20-residue protein and subsequently selected one every 30 residues, reaching a total of seven protein structures. For proteins

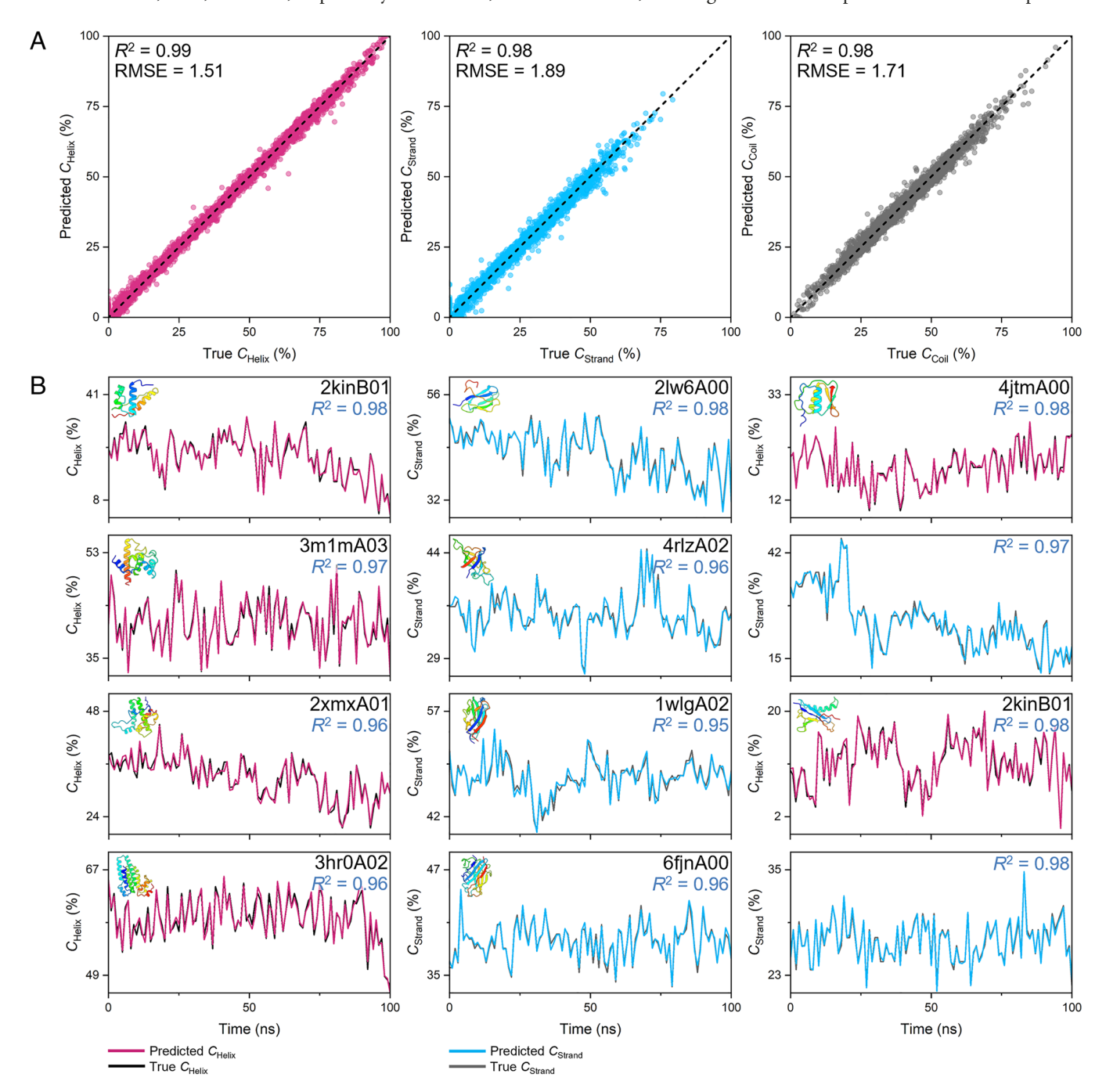


Fig. 2. Pretraining results on the CATH dataset. (A) Sequential scatter plots showing predictions for helix, strand, and coil contents, arranged from left to right. (B) Predictions for the dynamic secondary structure contents across three classes of protein trajectories: "mainly helix," "mainly strand," and mixed "helix/strand."

with more than 200 amino acid residues, we chose three proteins with about 250, 300, and 350 residues, to ensure a diverse and representative sampling from the original database. In Fig. 2B, for the three classes of proteins comprising approximately 80 to 170 amino acid residues, the pretrained model precisely predicts the dynamic content changes of the secondary structures, achieving an R^2 value of at least 0.95. From the complete predictions for the 30 trajectories depicted in *SI Appendix*, Fig. S4, there is an overall decreasing trend in the predictive performance of the model as the number of residues is incrementally raised from ~20 to 350, which is correlated with the overlap of the oscillator signals in the 2DIR spectra (45). Notably, even for the trajectory of a protein with up to 382 residues (CATH ID: 506hA00), the model still maintains good predictions with an R^2 value of at least 0.91. These findings demonstrate the effectiveness of our pretrained model in capturing the intricacies of 2DIR spectra, enabling it to provide accurate and reliable predictions on the secondary structure content of corresponding protein conformations.

Transfer Learning for Tracing Protein Folding Trajectories. In the previous section, the spectrum-structure dataset constructed through MD simulations is confined to the nanosecond scale due to computational constraints. However, protein folding processes typically occur over the microsecond to millisecond timescale (46, 47). The potential of our pretrained model to successfully transfer to datasets with broader timescales will thus be most valuable. As shown in Fig. 3, the reversible folding trajectories of four proteins with distinct secondary structure characteristics, simulated on the Anton supercomputer (48, 49), were utilized to evaluate the transferability of our model. Specifically, Trp-cage (PDB ID: 2JOF)

and $\alpha3D$ (PDB ID: 2A3D) contain only helices, WW domain (PDB ID: 2F21) consists solely of strands (50), and ubiquitin (PDB ID: 1UBQ) features a mixture of both (51). For each complete folding trajectory, approximately 10,000 conformations were harvested at equal time intervals. The first 40% of this dataset was allocated for fine-tuning to update the pretrained weights, and this portion was randomly divided into training and validation sets in a 9:1 ratio. The remaining 60% served as the test set to verify transfer performance. The correlation curves between the predictive performance and the amount of fine-tuning data in the training set for different proteins are detailed in *SI Appendix*, Fig. S5 and Table S1.

For the Trp-cage folding trajectory in Fig. 3A, the prediction results of the test set start at 80 µs (see SI Appendix, Fig. S6 for the complete folding trajectory). Here, high or low variations in the helix content, correspond to the Trp-cage protein in a folded or unfolded state, respectively. Alternating folding and unfolding events can be clearly observed within the predicted 120-μs trajectory. The pretrained model, which was not fine-tuned using any 2DIR spectra, had an R^2 value of only 0.92 on the validation set. The predictive accuracy improves with the increasing amount of feeding data. Notably, when the amount of data reaches ~1800, an optimal performance is achieved, with R^2 value equals to 0.98 (SI Appendix, Fig. S5A). We highlighted five characteristic conformations marked by significant helix content variations and zoomed in to display the prediction details at surrounding times. These results reveal that our model can precisely trace the dynamic secondary structure content changes of Trp-cage along its folding process. The helices of the shown conformations are colored in red to enhance the visual representation, whereas the tertiary structures were not

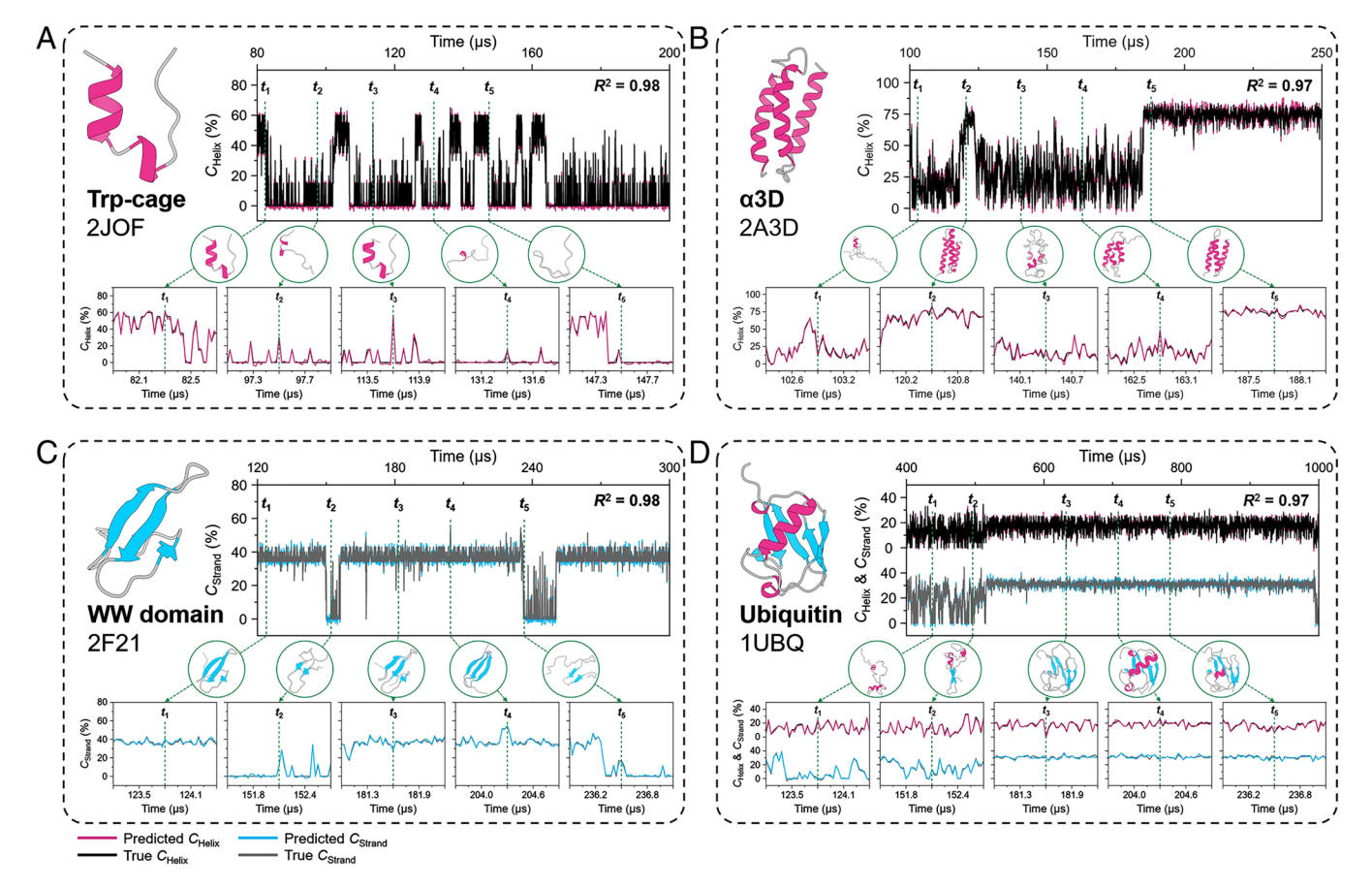


Fig. 3. Transfer learning results of protein folding trajectories simulated on the Anton supercomputer. Panels (A), (B), (C), and (D) correspond to the prediction results of Trp-cage, α 3D, WW domain, and ubiquitin, respectively. In each panel, we highlight five conformations with significant changes in secondary structure contents, labeled t_1 – t_5 , and further display prediction details at surrounding times.

predicted. The α3D protein, similar to Trp-cage in containing only helices, possesses about three times the number of amino acid residues, leading to more complex 2DIR signals. At the same time, folding and unfolding events are less frequent within the prediction time span (Fig. 3B), increasing the prediction challenge. However, even without fine-tuning, the model provides an R^2 value of 0.84. Increasing the fine-tuning data to \sim 3,000 led to satisfactory predictions, with R^2 value reaching 0.97 (SI Appendix, Fig. S5B). The WW domain primarily consists of strand-type secondary structures. The 2DIR spectral features associated with strands were effectively captured during the previous pretraining step, facilitating quite a smooth transfer learning process. The R^2 values before and after fine-tuning were 0.90 and 0.98, respectively, with a fine-tuning data usage of ~2,400 (Fig. 3C and SI Appendix, Fig. S5C). Ubiquitin, widely found in eukaryotic cells, has 76 amino acid residues and features both helix and strand secondary structures. Fig. 3D shows that our fine-tuned model can accurately predict the helices and strands content changes for each conformation throughout the folding process. Upon using nearly all of the spectra from the training set, the R^2 value increased from 0.85 to 0.97 (SI Appendix, Fig. S5D). It is noteworthy that the CHARMM22* force field slightly underestimates the stability of helices in the folded state of ubiquitin (52), leading to a greater variance in helix content compared to the strand. After the model was pretrained on a vast and varied spectral dataset to optimize its weights, only a minimal amount of additional data was required for fine-tuning to achieve exceptional predictive accuracy on entirely new datasets. Please note that for these four trajectories, training the same model from scratch resulted in the R^2 values of only 0.71, 0.67, 0.67, and 0.63, respectively (*SI Appendix*, Table S1). We thus believe that this pretrained model can facilitate universal transfer learning for predicting the dynamic

secondary structure content changes of protein trajectories. The code and weights files of our model are freely accessible on our GitHub repository (53) (https://github.com/SaintCloud-0013/2DIR-ML), and future downloads and verifications are highly appreciated.

Attention-Based Interpretation of Spectral Signals. Beyond its universal transfer learning capability, our model offers a significant advantage by providing visual interpretations on the original spectra for its prediction results. By analyzing the attention maps corresponding to different secondary structures, we gain insights into the characteristic regions of 2DIR spectra that the model focuses on when making predictions. After integrating the attention weights across all the MSA layers (54), Fig. 4 provides the digital interpretation of the model for ubiquitin conformations during its folding process. Sequentially displayed from top to bottom are the corresponding 2DIR spectra, helix attention maps, and strand attention maps. It is evident that the transition signals at different vibrational energy levels are effectively captured (in the 2DIR spectra, blue and red denote transitions of the vibrational quantum numbers $v = 0 \rightarrow 1$ and $v = 1 \rightarrow 2$, respectively). Both diagonal and off-diagonal (cross) peak regions contribute to the structure identification (33). There is a clear distinction in the attention distribution for the helix and strand. The model focuses primarily on the spectral region around 1,650 cm⁻¹ for the helix, while for the strand, the attention is mainly on the region around 1,630 cm⁻¹, with a minor contribution around 1,680 cm⁻¹. This observation aligns with generally accepted understanding (55), suggesting that the model effectively captures the relevant features from the original 2DIR spectra during its learning process. In addition, we find that as the helix content increases, the corresponding attention undergoes a redshift, a similar redshift is noted with an increase in strand

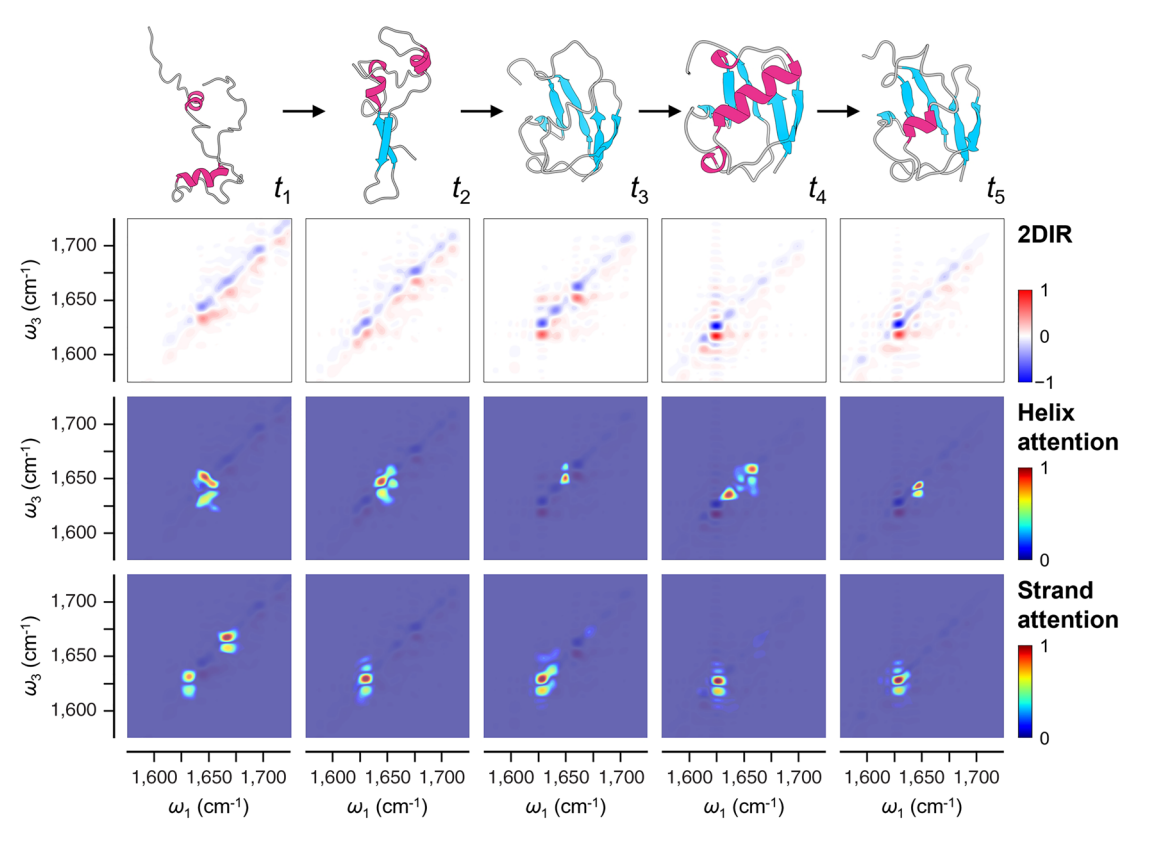


Fig. 4. Attention maps of different secondary structures for ubiquitin conformations. The figure displays, from top to bottom, the conformations along the ubiquitin folding trajectory, followed by the corresponding 2DIR spectra, helix attention maps, and strand attention maps.

content, consistent with previous work (56–59). This attention-based spectral interpretation enhances the transparency of the ML black box, fostering greater trust in the pretrained model and making it more reliable and effective for practical applications.

Discussion

In summary, we have developed a pretrained ML model based on the state-of-the-art transformer architecture, which captures features of 2DIR spectra and establishes a spectrum-structure correlation. This facilitates a universal prediction of dynamic secondary structure content changes along protein trajectories. During the pretraining phase, about 204,300 2DIR spectra were used to optimize the model weights. The pretrained model demonstrates high fidelity in predicting helix, strand, and coil contents of protein conformations in the validation set, with coefficient of determination R^2 values of 0.99, 0.98, and 0.98, respectively. Remarkably, in the transfer learning process, even without fine-tuning, the model still achieved fair R^2 values over 0.84 in predicting dynamic content changes for real folding trajectories of four typical proteins, namely Trp-cage, α 3D, WW domain, and ubiquitin. Following a time-efficient and dataminimal fine-tuning step, R^2 values reached satisfactory 0.98, 0.97, 0.98, and 0.97, respectively, underscoring its universal transferability and high performance. Moreover, the model can provide an attention-based interpretation of spectroscopic signals by elucidating the dynamics of different secondary structures along protein trajectories. By using 2DIR spectroscopy to trace conformational structures during protein dynamics, this model can provide useful insights into the dynamic behavior of proteins in their biological functions. With the significant boost in computing power, the pretraining protocol detailed in this article should provide a powerful methodology for the protein dynamics community, and trigger the development and applications of ML models in related fields.

Materials and Methods

As described in the previous sections, 2DIR spectra can serve as a tool for tracing the dynamic conformations of proteins. However, extracting oscillator signals from these spectra and converting them into quantitative structural information presents a major challenge. Our aim is to establish a spectrum-structure correlation

"Mainly Alpha," "Mainly Beta," and "Alpha Beta." The complete index of files can be found in SI Appendix. To capture the dynamic conformations, MD simulations were conducted for each protein using the Gromacs (60) software, with detailed settings provided below. For each trajectory, 50 snapshots were harvested at 1-ns intervals following the NVT and NPT equilibria. The entire pretraining dataset comprises a total of $4,086 \times 50 = 243,000$ spectra. The transfer learning dataset features protein reversible folding trajectories, simulated on the Anton supercomputer across timescales from microseconds to milliseconds. This collection encompasses structures such as the Trp-cage, α 3D, WW domain, and ubiquitin. For each trajectory, we sampled approximately 10,000 conformations at equal time intervals to compute the 2DIR spectra. The secondary structure assignments for protein conformations were determined by calculating hydrogen bond energies (61) anrd mainchain dihedral angles from the atomic coordinates of the snapshots, using the Stride (42) program.

2DIR spectra simulations. We employed the Frenkel exciton Hamiltonian within the amide I spectral window:

$$\mathbf{H} = \sum_{i}^{N} \omega_{i} \boldsymbol{b}_{i}^{\dagger} \boldsymbol{b}_{i} + \sum_{i,j}^{N} J_{ij} \boldsymbol{b}_{i}^{\dagger} \boldsymbol{b}_{j} - \sum_{i}^{N} \frac{\Delta_{i}}{2} \boldsymbol{b}_{i}^{\dagger} \boldsymbol{b}_{j}^{\dagger} \boldsymbol{b}_{i} \boldsymbol{b}_{i}.$$

Here, b_i^{\dagger} and b_i represent the Bosonic creation and annihilation operators for individual peptide unit, respectively. ω_i is the vibrational frequency of the local mode, J_{ij} denotes the coupling between two local modes, and Δ_i refers to the anharmonicity. The frequency of an oscillator is calculated using the Skinner map (62), where the environment of the C and N atoms is considered:

$$\omega = \omega_{map} + \sum_{i} P_{i,map} P_i + (\mathbf{E}_{i,map} \cdot \mathbf{E}_i).$$

 ω_{map} , $P_{i,map}$, and $\mathbf{E}_{i,map}$ are, respectively, the vibrational frequency, electric potential, and electric field, as predefined in the map. P_i and \mathbf{E}_i were computed as follows:

$$P = \sum_{j} \frac{q_{j}}{|\mathbf{r}_{j}|},$$

$$E_{x} = \sum_{i} \frac{q_{j}}{|\mathbf{r}_{i}|^{3}} (\mathbf{r}_{j} \cdot \widehat{\mathbf{x}}).$$

 E_x is the electric field in the x-direction, E_y and E_z can be calculated in a similar manner. Additionally, frequency shifts for each neighboring amide groups are incorporated based on Ramachandran angles (63).

The coupling between the neighboring and nonneighboring oscillators is determined through the transition charge coupling (TCC) (64) and glycine dipeptide (GLDP) methods (65), respectively:

$$J = \frac{1}{4\pi\varepsilon} \sum_{a,b} \left(\frac{dq_a dq_b}{|\mathbf{r}_{ab}|} - \frac{3q_a q_b (\mathbf{v}_a \cdot \mathbf{r}_{ab}) (\mathbf{v}_b \cdot \mathbf{r}_{ab})}{|\mathbf{r}_{ab}|^5} - \frac{dq_a q_b (\mathbf{v}_b \cdot \mathbf{r}_{ab}) - q_a dq_b (\mathbf{v}_a \cdot \mathbf{r}_{ab}) - q_a q_b (\mathbf{v}_a \cdot \mathbf{v}_b)}{|\mathbf{r}_{ab}|^3} \right)$$

$$J = (1 - u)(1 - t) \cdot map\left(\left\lfloor \frac{\phi}{30} \right\rfloor \left\lfloor \frac{\phi}{30} \right\rfloor \right) + (1 - u)t \cdot map\left(\left\lfloor \frac{\phi}{30} \right\rfloor \left\lfloor \frac{\psi}{30} \right\rfloor \right) + u(1 - t) \cdot map\left(\left\lfloor \frac{\phi}{30} \right\rfloor \left\lfloor \frac{\psi}{30} \right\rfloor \right) + u \cdot t \cdot map\left(\left\lfloor \frac{\phi}{30} \right\rfloor \left\lfloor \frac{\psi}{30} \right\rfloor \right).$$

through ML, facilitating the prediction of protein secondary structure contents. Additionally, by leveraging pretraining techniques in combination with a vast and varied dataset, we strive to achieve universal transferability across various protein folding trajectories.

Dataset Construction. The 2DIR spectra used in both the pretraining and transfer learning datasets were generated through simulations derived from protein PDB files. The computational protocol of these spectra is detailed below. The initial structures for constructing the pretraining dataset were sourced from the CATH database v4.3 (37), developed by Orengo et al. This database is organized according to the protein secondary structure categories. From it, we extracted 4,086 distinct homologous superfamily protein structures using three major categories:

The dipole moment of each oscillator was obtained from the relative positions between C, O, and N atoms (66):

$$\mu = 2.73(\mathbf{s} - ((\mathbf{CO} \cdot \mathbf{s}) + \frac{\sqrt{|\mathbf{s}|^2 - (\mathbf{CO} \cdot \mathbf{s})^2}}{\tan 10})\mathbf{CO}).$$

The 2DIR spectrum is the imaginary part of the sum of the rephasing (photon echo, $\mathbf{k}_1 = -\mathbf{k}_1 + \mathbf{k}_2 + \mathbf{k}_3$) and nonrephasing signals ($\mathbf{k}_{11} = \mathbf{k}_1 - \mathbf{k}_2 + \mathbf{k}_3$), where \mathbf{k}_1 , \mathbf{k}_2 , and \mathbf{k}_3 are the wave vectors of the incoming infrared fields with time delays of t_1 , t_2 , and t_3 .

$$I_{2D}(\omega_3, t_2, \omega_1) = Im(S^{(1)}(\omega_3, t_2, \omega_1) + S^{(1)}(\omega_3, t_2, \omega_1)),$$

$$\begin{split} S^{(l)}(\omega_{3},t_{2},\omega_{1}) &= \int_{0}^{\infty} \int_{0}^{\infty} (S_{\text{GB}}^{(l)}(t_{3},t_{2},t_{1}) + S_{\text{SE}}^{(l)}(t_{3},t_{2},t_{1}) \\ &+ S_{\text{EA}}^{(l)}(t_{3},t_{2},t_{1})) exp(i(\omega_{3}t_{3} - \omega_{1}t_{1})) dt_{3} dt_{1}, \\ S^{(ll)}(\omega_{3},t_{2},\omega_{1}) &= \int_{0}^{\infty} \int_{0}^{\infty} (S_{\text{GB}}^{(l)}(t_{3},t_{2},t_{1}) + S_{\text{SE}}^{(l)}(t_{3},t_{2},t_{1}) \\ &+ S_{\text{EA}}^{(l)}(t_{3},t_{2},t_{1})) exp(i(\omega_{3}t_{3} + \omega_{1}t_{1})) dt_{3} dt_{1}, \end{split}$$

where ω_1 and ω_3 represent the frequencies of t_1 and t_3 after Fourier transformation, respectively. GB, SE, and EA represent the contributions from different Liouville space pathways, known as ground-state bleach, stimulated emission and excited-state absorption, respectively.

MD simulations. The protein PDB entries within the CATH database, were subjected to MD sampling using Gromacs 2018. In the aqueous environment, the all-atom OPLS-AA/L force field was utilized in combination with TIP3P water molecules, and Na⁺ or Cl⁻ ions were used to balance the charge of the system. To avoid the influence of periodic images, the protein molecule was centrally positioned in a cubic box, ensuring at least 1.0 nm distance from the edges. A 50,000-step energy minimization was applied to eliminate steric clashes or inappropriate geometries. This was followed by two-phases NVT and NPT equilibration steps, each lasting 100 ps. Production dynamics was then performed for a period of 50 ns with a 2-fs timestep. The system was maintained at 373 K and 1 atmosphere using v-rescale Berendsen thermostat (67) and Parrinello-Rahman barostat (68), respectively. Fifty snapshots were collected every 1 ns along each production trajectory.

Model Architecture. In the 2DIR spectra, information on frequencies and couplings of vibrational modes is stored in a contour plot with excitation frequency (ω_1) and detection frequency (ω_3) serving as the coordinate axes. A self-attention-based transformer is adopted to capture the features of these two-dimensional matrices. The model primarily consists of three components: segmented embeddings of 2DIR matrices, a backbone network of Transformer Encoder, and an MLP head for regression tasks. The input 2DIR signals covering the 1,575 to 1,725 cm⁻¹ spectral window are resized to 224×224 matrices and then segmented into 16×16 small patches. Each patch is linearly embedded into the network, incorporating position embeddings and an extra learnable regression [RGS] token for numerical regression of the secondary structure contents. The Transformer Encoder comprises 12 alternating sets of MSA and MLP layers, with LN technique being utilized. The [RGS] token, processed by the Transformer Encoder, captures the essential spectral features of 2DIR signal. It then proceeds through an MLP layer to predict the secondary structure contents of protein conformations.

- G. Brändén, R. Neutze, Advances and challenges in time-resolved macromolecular crystallography. Science 373, eaba0954 (2021)
- S. Ahlawat, K. R. Mote, N. A. Lakomek, V. Agarwal, Solid-state NMR: Methods for biological solids. Chem. Rev. 122, 9643-9737 (2022).
- Y. Cheng, Single-particle cryo-EM-How did it get here and where will it go. Science 361, 876-880 (2018).
- J. Jumper et al., Highly accurate protein structure prediction with AlphaFold. Nature 596, 583-589 (2021).
- K. Tunyasuvunakool et al., Highly accurate protein structure prediction for the human proteome. Nature 596, 590-596 (2021).
- M. Baek et al., Accurate prediction of protein structures and interactions using a three-track neural network. Science 373, 871-876 (2021).
- I. R. Humphreys et al., Computed structures of core eukaryotic protein complexes. Science 374, eabm4805 (2021).
- J. Dauparas et al., Robust deep learning-based protein sequence design using ProteinMPNN. Science 378, 49-56 (2022).
- human nuclear pores. Science 376, eabm9506 (2022).
- A. Fryszkowska et al., A chemoenzymatic strategy for site-selective functionalization of native peptides and proteins. Science 376, 1321-1327 (2022).
- I. D. Lutz et al., Top-down design of protein architectures with reinforcement learning. Science 380, 266-273 (2023).
- M. L. Hekkelman, I. de Vries, R. P. Joosten, A. Perrakis, AlphaFill: Enriching AlphaFold models with ligands and cofactors. Nat. Methods 20, 205-213 (2023).
- J. Abramson et al., Accurate structure prediction of biomolecular interactions with AlphaFold 3. Nature, in press. https://doi.org/10.1038/s41586-024-07487-w.
- R. Krishna et al., Generalized biomolecular modeling and design with RoseTTAFold All-Atom Science 384, eadl2528 (2024)
- J. L. Watson et al., De novo design of protein structure and function with RFdiffusion. Nature 620, 1089-1100 (2023).
- J. B. Ingraham et al., Illuminating protein space with a programmable generative model. Nature 623, 1070-1078 (2023).

Pretraining and fine-tuning configurations. During the pretraining phase, we utilized the AdamW (69) optimizer, configured with a learning rate of 10⁻⁴ and a weight decay of 10^{-2} . The pretraining dataset was randomly divided into training and validation sets in an 8:2 ratio. The model was trained for 100 epochs with a batch size of 256. A learning rate warmup strategy was implemented for the initial 5% of the total epochs, followed by a linear decay to zero for the remaining.

For the fine-tuning step, pretrained model weights are loaded to optimize for predicting specific protein folding trajectory. The optimizer and learning rate strategy are consistent with the pretraining step, and the weights across all layers are updated. The 2DIR spectra calculated from the first 40% snapshots of the complete folding trajectory were used to construct the fine-tuning dataset, which was randomly split into training and validation sets in a ratio of 9:1. The remaining 60% is served as a test set to evaluate the performance of the fine-tuned model. Given the relatively small size of the dataset used for the fine-tuning, the model was trained with a batch size of 32 during 40 epochs.

Data, Materials, and Software Availability. Protein files with distinct secondary structure characteristics are available from the CATH database (37) (https:// www.cathdb.info/browse/tree). Protein folding trajectories are available from D. E. Shaw Research (50, 51) (https://www.deshawresearch.com/resources.html). Code is available at our GitHub repository (53) (https://github.com/SaintCloud-0013/2DIR-ML). All other data are included in the manuscript and/or supporting information.

ACKNOWLEDGMENTS. We thank David E. Shaw and his colleagues for providing data and assistance. This work was financially supported by Hefei Comprehensive National Science Center, the Innovation Program for Quantum Science and Technology (2021ZD0303303), the Chinese Academy of Sciences (CAS) Project for Young Scientists in Basic Research (YSBR-005), and the National Natural Science Foundation of China (22025304, 22033007, and 22303091). We thank the Hefei Advanced Computing Center for providing numerical computations; and the University of Science and Technology of China (USTC) Supercomputing Center for providing computational resources for this project. S.Y. acknowledges the support of the National Natural Science Foundation of China (22203001, 62236002, and 61921004), the University Synergy Innovation Program of Anhui Province (GXXT-2022-062), and the Natural Science Foundation of Anhui Province (2208085Y04). S.M. acknowledges the support of the National Science Foundation (CHE-2246379). S.M. is a senior fellow at the Hagler Institute for Advanced Study at Texas A&M University.

- 17. L. Lu et al., De novo design of drug-binding proteins with predictable binding energy and specificity. Science 384, 106-112 (2024).
- M. Baek et al., Accurate prediction of protein-nucleic acid complexes using RoseTTAFoldNA. Nat. Methods 21, 117-121 (2024).
- S. Bhatia, J. B. Udgaonkar, Heterogeneity in protein folding and unfolding reactions. *Chem. Rev.* 122, 8911-8935 (2022).
- H. K. Wayment-Steele et al., Predicting multiple conformations via sequence clustering and AlphaFold2. Nature 625, 832-839 (2024).
- W. Lu et al., DynamicBind: Predicting ligand-specific protein-ligand complex structure with a deep equivariant generative model. Nat. Commun. 15, 1071 (2024).
- E. Rennella, D. D. Sahtoe, D. Baker, L. E. Kay, Exploiting conformational dynamics to modulate the function of designed proteins. Proc. Natl. Acad. Sci. U.S.A. 120, e2303149120 (2023).
- S. Mukamel et al., Coherent multidimensional optical probes for electron correlations and exciton dynamics: From NMR to X-rays. Acc. Chem. Res. 42, 553-562 (2009).
- A. Ghosh, J. S. Ostrander, M. T. Zanni, Watching proteins wiggle: Mapping structures with twodimensional infrared spectroscopy. Chem. Rev. 117, 10726-10759 (2017).
- J. P. Kraack, P. Hamm, Surface-sensitive and surface-specific ultrafast two-dimensional vibrational spectroscopy. Chem. Rev. 117, 10623-10664 (2017).
- C. R. Baiz et al., Vibrational spectroscopic map, vibrational spectroscopy, and intermolecular interaction. Chem. Rev. 120, 7152-7218 (2020).
- N. T. Hunt, Using 2D-IR spectroscopy to measure the structure, dynamics, and intermolecular interactions of proteins in H2O. Acc. Chem. Res. 57, 685-692 (2024).
- H. T. Kratochvil et al., Instantaneous ion configurations in the K⁺ ion channel selectivity filter revealed by 2D IR spectroscopy. Science 353, 1040-1044 (2016).
- R. Hu et al., Ultrafast two-dimensional infrared spectroscopy resolved a structured lysine 159 on the cytoplasmic surface of the microbial photoreceptor bacteriorhodopsin. J. Am. Chem. Soc. 144, 22083-22092 (2022).
- M. J. Ryan, L. Gao, F. I. Valiyaveetil, A. A. Kananenka, M. T. Zanni, Water inside the selectivity filter of a K⁺ ion channel: Structural heterogeneity, picosecond dynamics, and hydrogen bonding J. Am. Chem. Soc. 146, 1543-1553 (2024)
- V. Barone et al., Computational molecular spectroscopy. Nat. Rev. Methods Primers 1, 38 (2021)

- P. Klukowski, R. Riek, P. Güntert, Rapid protein assignments and structures from raw NMR spectra with the deep learning technique ARTINA. Nat. Commun. 13, 6151 (2022).
- H. Ren et al., Machine learning recognition of protein secondary structures based on twodimensional spectroscopic descriptors. Proc. Natl. Acad. Sci. U.S.A. 119, e2202713119 (2022).
- P. Klukowski, R. Riek, P. Güntert, Time-optimized protein NMR assignment with an integrative deep learning approach using AlphaFold and chemical shift prediction. Sci. Adv. 9, eadi9323 (2023).
- T. Yang et al., Catalytic structure design by Al generating with spectroscopic descriptors. J. Am. Chem. Soc. 145, 26817–26823 (2023).
- A. Dosovitskiy et al., An image is worth 16×16 words: Transformers for image recognition at scale. arXiv [Preprint] (2020). https://doi.org/10.48550/arXiv.2010.11929 (Accessed 22 October 2020).
- I. Sillitoe et al., CATH: Increased structural coverage of functional space. Nucleic Acids Res. 49, D266-D273 (2021).
- H. Kim, M. Cho, Infrared probes for studying the structure and dynamics of biomolecules. Chem. Rev. 113, 5817–5847 (2013).
- B. Blasiak, C. H. Londergan, L. J. Webb, M. Cho, Vibrational probes: From small molecule solvatochromism theory and experiments to applications in complex systems. Acc. Chem. Res. 50, 968–976 (2017).
- T. Jansen, J. Knoester, Nonadiabatic effects in the two-dimensional infrared spectra of peptides: Application to alanine dipeptide. J. Phys. Chem. B 110, 22910–22916 (2006).
- T. L. Jansen, J. Knoester, Waiting time dynamics in two-dimensional infrared spectroscopy. Acc. Chem. Res. 42, 1405–1411 (2009).
- D. Frishman, P. Argos, Knowledge-based protein secondary structure assignment. Proteins 23, 566-579 (1995).
- R. Xiong et al., On layer normalization in the transformer architecture. arXiv [Preprint] (2020). https://doi.org/10.48550/arXiv.2002.04745 (Accessed 12 February 2020).
- L. Liu, X. Liu, J. Gao, W. Chen, J. Han, Understanding the difficulty of training transformers. arXiv [preprint] (2020). https://doi.org/10.48550/arXiv.2004.08249 (Accessed 17 April 2020).
- W. Zhuang, T. Hayashi, S. Mukamel, Coherent multidimensional vibrational spectroscopy of biomolecules: Concepts, simulations, and challenges. *Angew. Chem. Int. Ed.* 48, 3750–3781 (2009).
- H. S. Chung, K. McHale, J. M. Louis, W. A. Eaton, Single-molecule fluorescence experiments determine protein folding transition path times. *Science* 335, 981–984 (2012).
- 47. K. A. Dill, J. L. MacCallum, The protein-folding problem, 50 years on. Science 338, 1042–1046 (2012).
- D. E. Shaw et al., Atomic-level characterization of the structural dynamics of proteins. Science 330, 341–346 (2010).
- D. E. Shaw et al., "Millisecond-scale molecular dynamics simulations on Anton" in SC'09: International Conference for High Performance Computing, Networking, Storage and Analysis (ACM, 2009), pp. 1–11.
- K. Lindorff-Larsen, S. Piana, R. O. Dror, D. E. Shaw, How fast-folding proteins fold. Science 334, 517–520 (2011).
- S. Piana, K. Lindorff-Larsen, D. E. Shaw, Atomic-level description of ubiquitin folding. Proc. Natl. Acad. Sci. U.S.A. 110, 5915–5920 (2013).

- S. Piana, K. Lindorff-Larsen, D. E. Shaw, How robust are protein folding simulations with respect to force field parameterization? *Biophys. J.* 100, L47–49 (2011).
- F. Wu et al., Unraveling dynamic protein structures by two-dimensional infrared spectra with a pretrained machine learning model. Github. Available at https://github.com/SaintCloud-0013/2DIR-ML. Deposited 2 May 2024.
- S. Abnar, W. Zuidema, Quantifying attention flow in transformers. arXiv [Preprint] (2020). https://doi.org/10.48550/arXiv.2005.00928 (Accessed 2 May 2020).
- M. D. Fayer, Ultrafast Infrared Vibrational Spectroscopy (Taylor & Francis, Boca Raton, FL, 2013), p. 475.
- Z. Ganim et al., Amide I two-dimensional infrared spectroscopy of proteins. Acc. Chem. Res. 41, 432-441 (2008).
- Z. Lai, N. K. Preketes, S. Mukamel, J. Wang, Monitoring the folding of Trp-cage peptide by twodimensional infrared (2DIR) spectroscopy. *J. Phys. Chem. B* 117, 4661-4669 (2013).
- H. S. Chung, M. Khalil, A. W. Smith, Z. Ganim, A. Tokmakoff, Conformational changes during the nanosecond-to-millisecond unfolding of ubiquitin. *Proc. Natl. Acad. Sci. U.S.A.* 102, 612-617 (2005)
- H. S. Chung, Z. Ganim, K. C. Jones, A. Tokmakoff, Transient 2D IR spectroscopy of ubiquitin unfolding dynamics. Proc. Natl. Acad. Sci. U.S.A. 104, 14237–14242 (2007).
- M. J. Abraham et al., GROMACS: High performance molecular simulations through multi-level parallelism from laptops to supercomputers. SoftwareX 1-2, 19-25 (2015).
- W. Kabsch, C. Sander, Dictionary of protein secondary structure: Pattern recognition of hydrogenbonded and geometrical features. *Biopolymers* 22, 2577–2637 (1983).
- L. Wang, C. T. Middleton, M. T. Zanni, J. L. Skinner, Development and validation of transferable amide I vibrational frequency maps for peptides. J. Phys. Chem. B 115, 3713–3724 (2011).
- T. Ia Cour Jansen, A. G. Dijkstra, T. M. Watson, J. D. Hirst, J. Knoester, Modeling the amide I bands of small peptides. J. Chem. Phys. 125, 44312 (2006).
- P. Hamm, S. Woutersen, Coupling of the amide I modes of the glycine dipeptide. Bull. Chem. Soc. Japan 75, 985–988 (2002).
- R. D. Gorbunov, D. S. Kosov, G. Stock, Ab initio-based exciton model of amide I vibrations in peptides: Definition, conformational dependence, and transferability. J. Chem. Phys. 122, 224904 (2005).
- H. Torii, M. Tasumi, Ab initio molecular orbital study of the amide I vibrational interactions between the peptide groups in di- and tripeptides and considerations on the conformation of the extended helix. J. Raman Spectrosc. 29, 81–86 (1998).
- G. Bussi, D. Donadio, M. Parrinello, Canonical sampling through velocity rescaling. J. Chem. Phys. 126. 014101 (2007).
- M. Parrinello, A. Rahman, Polymorphic transitions in single crystals: A new molecular dynamics method. J. Appl. Phys. 52, 7182–7190 (1981).
- I. Loshchilov, F. Hutter, Decoupled weight decay regularization. arXiv [Preprint] (2017). https://doi. org/10.48550/arXiv.1711.05101 (Accessed 14 November 2017).



Supporting Information for

Unravelling dynamic protein structures by two-dimensional infrared spectra with a pre-trained machine learning model

Fan Wu, Yan Huang, Guokun Yang, Sheng Ye*, Shaul Mukamel*, and Jun Jiang*

Corresponding authors: Sheng Ye, <u>yess@mail.ustc.edu.cn</u>; Shaul Mukamel, <u>smukamel@uci.edu</u>; Jun Jiang, <u>jiangj1@ustc.edu.cn</u>

This PDF file includes:

Figs. S1 to S6 Tables S1 SI References

Other supporting materials for this manuscript include the following:

Data S1 (separate file)

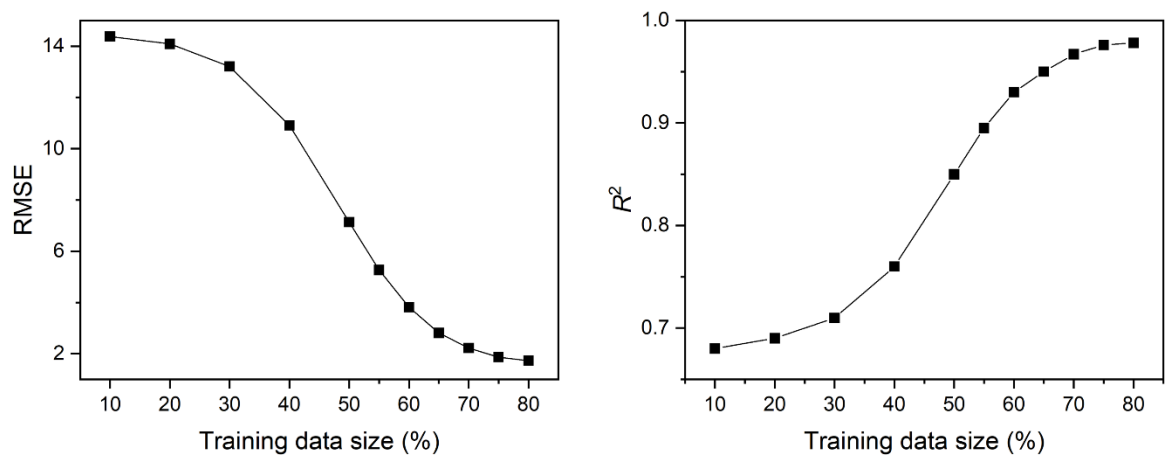


Fig. S1. Correlation between RMSE (left)/ R^2 value (right) and training data size during pre-training. The percentages on the x-axis represent the proportion of the training set size relative to the total dataset of 204,300.

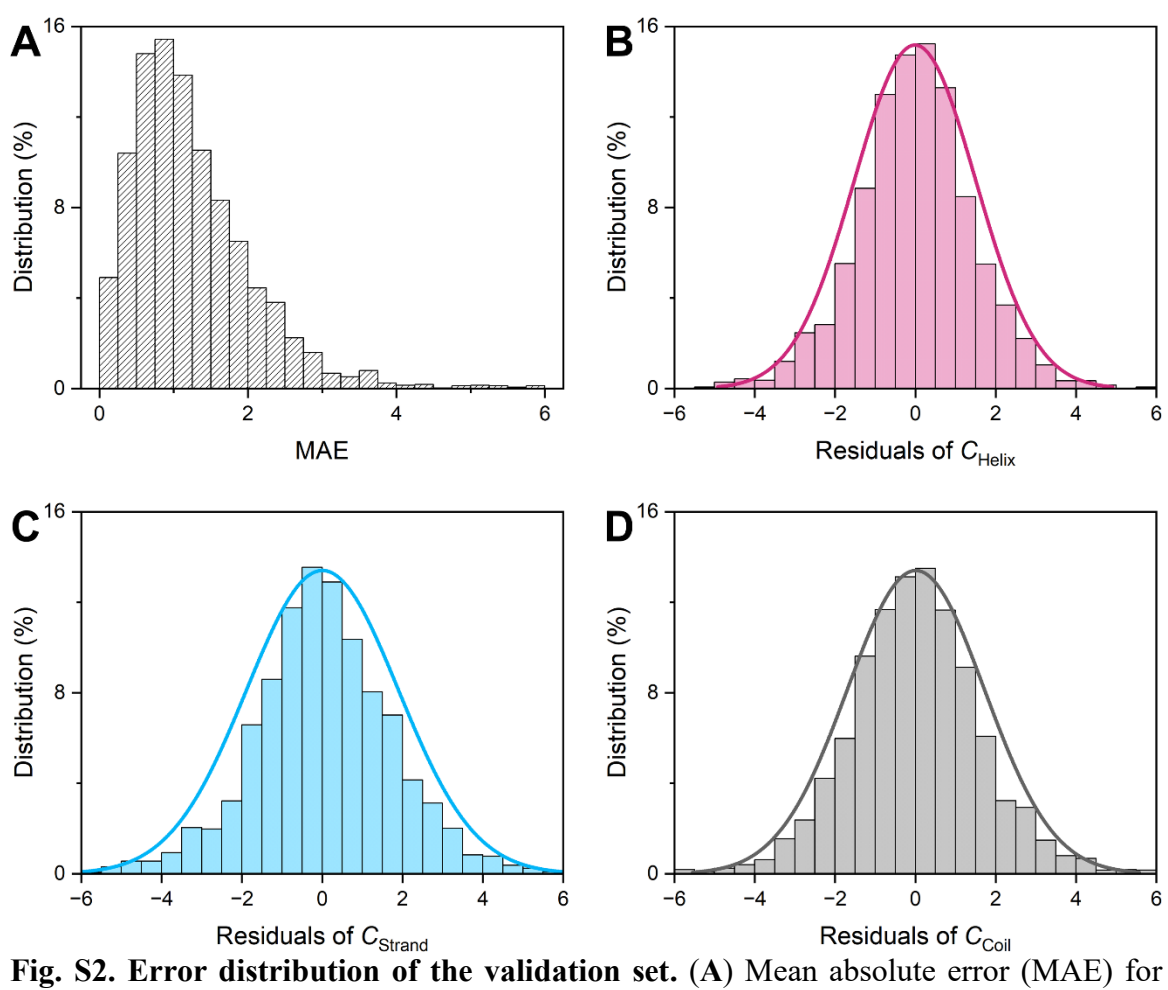


Fig. S2. Error distribution of the validation set. (A) Mean absolute error (MAE) for predicted secondary structure contents of protein conformations. Panels (B), (C), and (D) correspond to the residual distributions for the predicted contents of helix, strand, and coil, respectively.

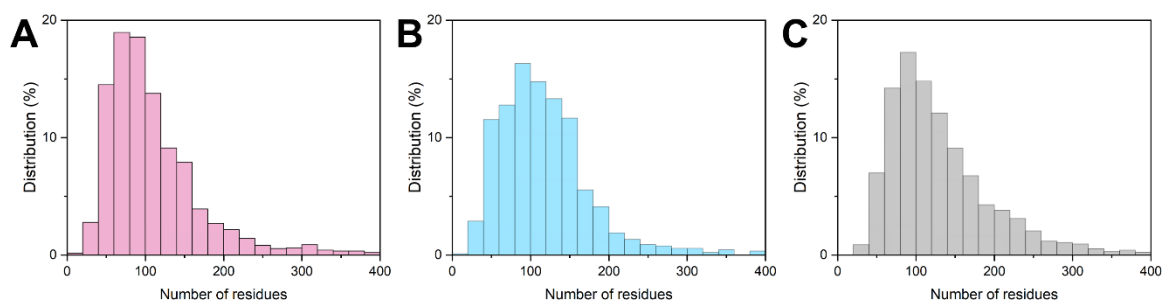


Fig. S3. Distribution of protein structures in the CATH databases, according to the number of amino acid residues. Panels (A), (B), and (C) correspond to the three major structural classes: "mainly helix", "mainly strand", and mixed "helix/strand", respectively. It can be seen that a large proportion of proteins in the database consist of less than 200 amino acid residues.

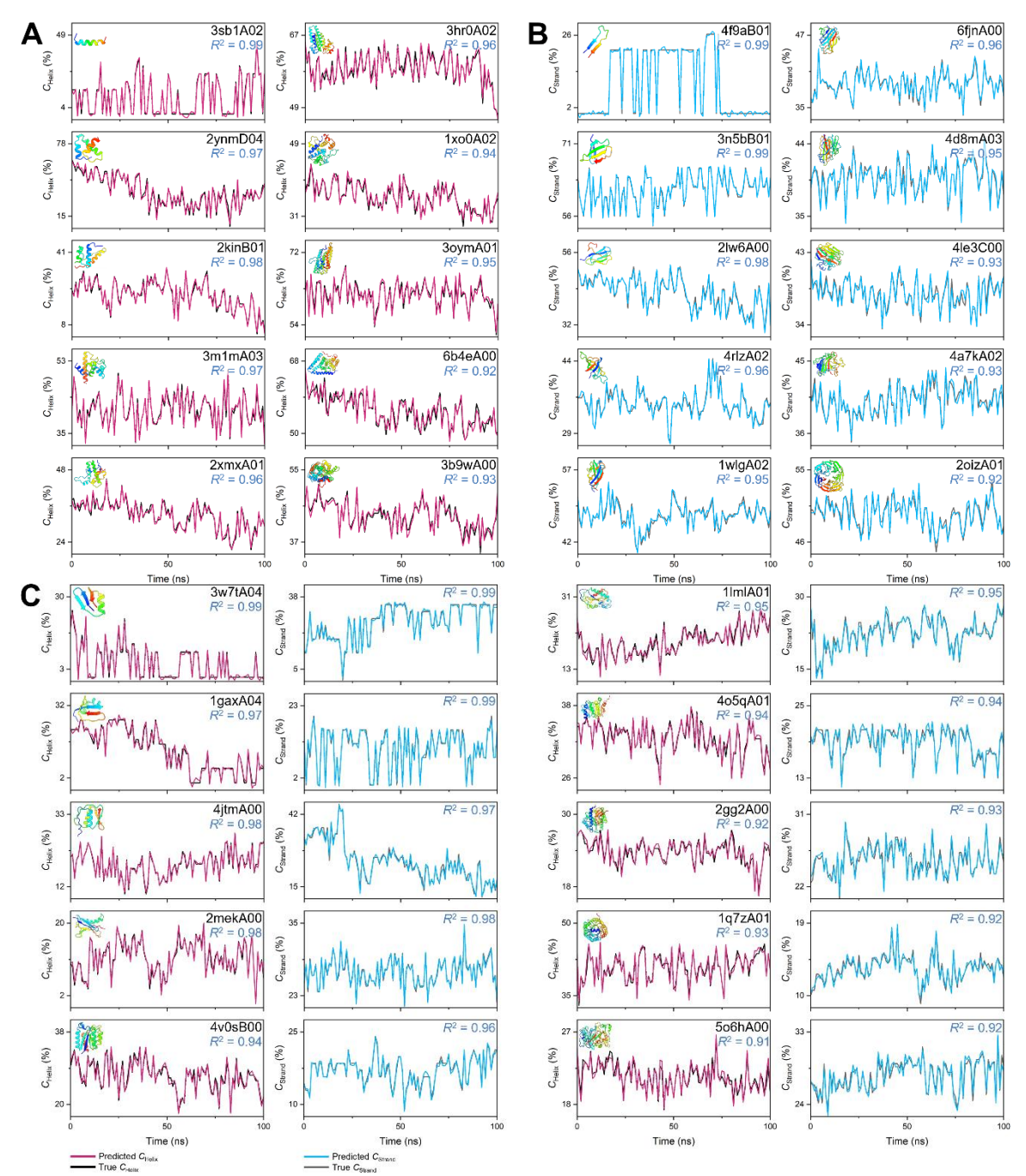


Fig. S4. Prediction results of dynamic secondary structure contents for protein trajectories in the CATH database. Panels (A), (B), and (C) correspond to the three major structural classes: "mainly helix", "mainly strand", and mixed "helix/strand", respectively. In each column, the amino acid residues of the proteins increase from top to bottom.

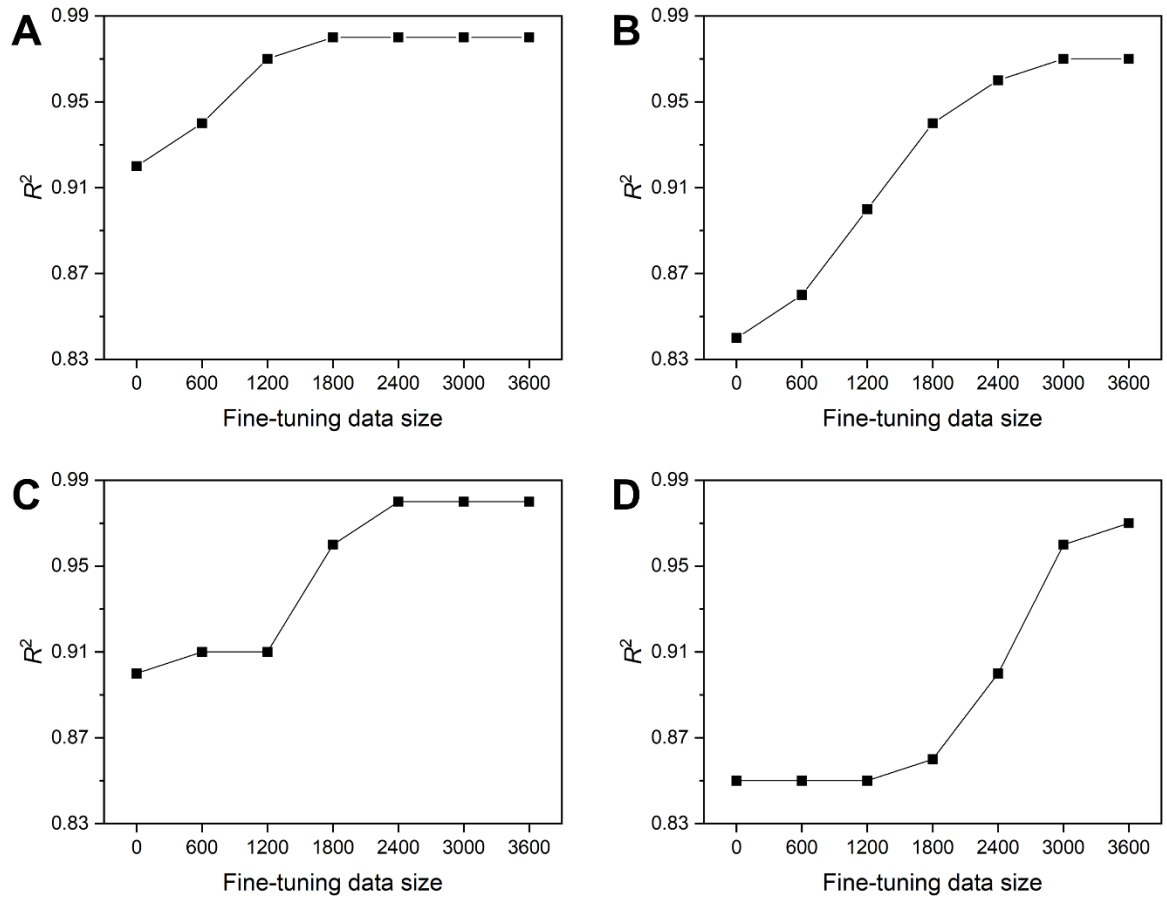


Fig. S5. Correlation between transfer learning performance and fine-tuning data size across different protein folding trajectories. Panels (A), (B), (C), and (D) correspond to the predicted R^2 values for the Trp-cage, α 3D, WW domain, and ubiquitin systems, respectively.

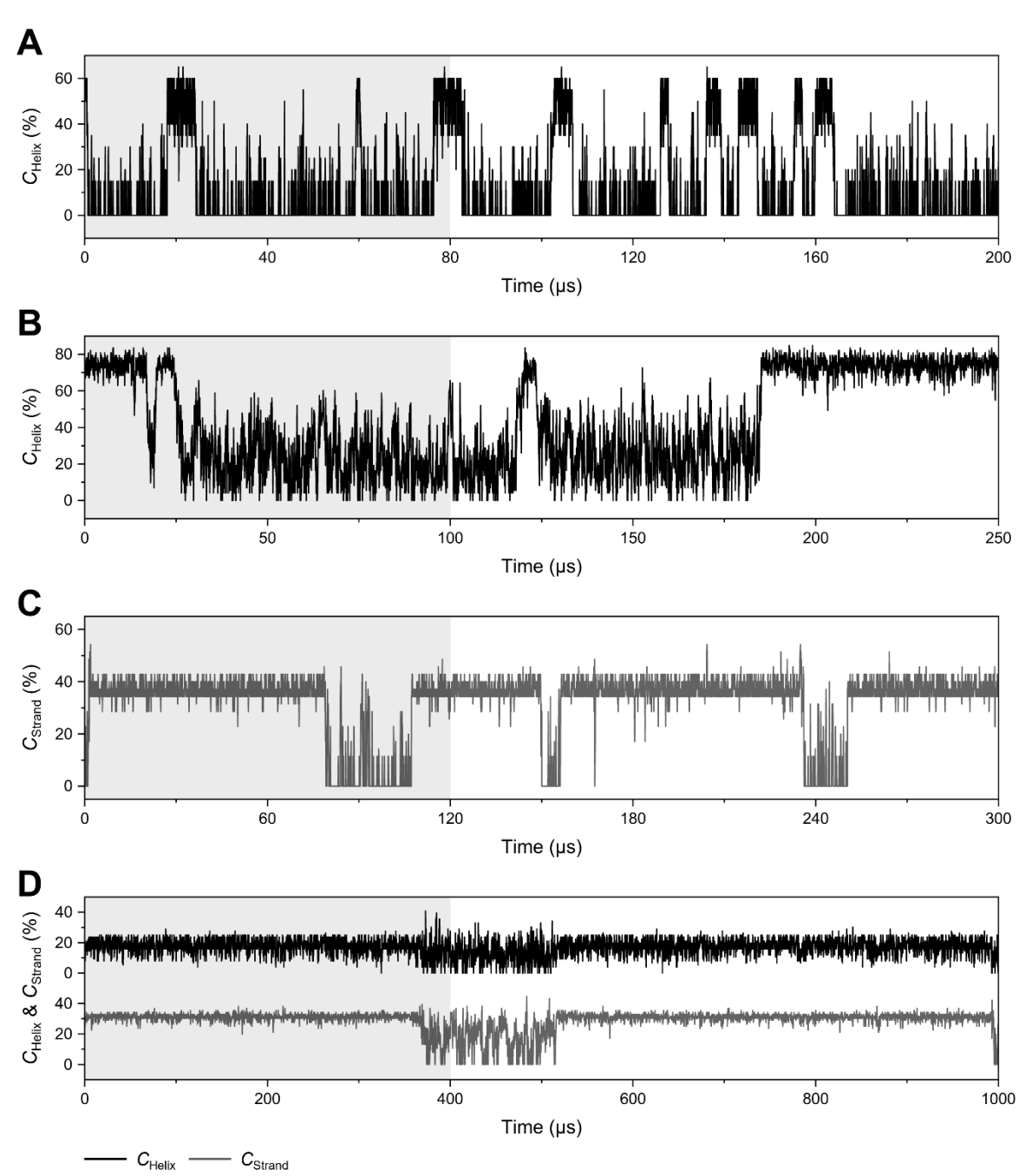


Fig. S6. Complete protein folding trajectories simulated on the Anton supercomputer. Panels (A), (B), (C), and (D) correspond to the folding trajectories of Trp-cage, α 3D, WW domain, and ubiquitin, respectively. In each trajectory, the area shaded in gray represent the training and validation sets, while the remaining is the test set.

Table S1. Transfer learning performance on protein folding trajectories simulated using the Anton supercomputer.

Protein name	PDB ID	Number of	umber of R ² without Fine-tuned Fine-tuning		R ² trained	Trajectory	
		residues	fine-tuning	R^2	data size	from scratch	references
Trp-cage	2JOF	20	0.92	0.98	~1800	0.71	(1)
α3D	2A3D	73	0.84	0.97	~3000	0.67	(1)
WW domain	2F21	35	0.90	0.98	~2400	0.67	(1)
Ubiquitin	1UBQ	76	0.85	0.97	~3600	0.63	(2)

Data S1. (separate file)

Protein entries used in the CATH database.

SI References

- 1. K. Lindorff-Larsen, S. Piana, R. O. Dror, D. E. Shaw, How fast-folding proteins fold. *Science* **334**, 517–520 (2011).
- 2. S. Piana, K. Lindorff-Larsen, D. E. Shaw, Atomic-level description of ubiquitin folding. *Proc. Natl. Acad. Sci. U. S. A.* **110**, 5915–5920 (2013).

1a0rP02	1a9xA04	1af7A01	1aq5A00	1av1A00	1avoA00	1b25A03	1b3qA01	1bg1A01	1bgfA00
1bhaA00	1bpoA02	1bvp101	1bvp103	1bzkA00	1c17M00	1c1kA02	1ciiA01	1cipA02	1cmbA00
1colA00	1dc1A02	1dd3A01	1dd9A03	1dekA02	1dgwY01	1dk8A01	1dquA02	1dvkA00	1e1hB01
1e5wA04	1e7lA02	1e7uA03	1ed1A00	1ehsA00	1ekeB02	1el6A01	1enwA00	1epuA03	1erdA00
1euvA01	1ezjA01	1ezjA02	1f0lB02	1f1mA00	1f5nA01	1f6vA00	1ffyA03	1fjkA00	1fs0G02
1g8eB00	1gaxA05	1gk9A01	1gk9A02	1gk9B03	1gkmA02	1gm5A01	1gmjD00	1gnlA01	1gqeA01
1gs9A00	1gxlA01	1gzsB00	1h5wB01	1h6uA01	1he1A00	1heiA03	1hgvA00	1hj0A00	1ho8A02
1hw7A02	1i5jA00	1iieA00	1iioA00	1iipA02	1ijyA00	1ik7A00	1iqvA00	1irqA00	1irxA04
1iuqA01	1iv8A03	1iv8A04	1ix9A01	1iyrA00	1izmA00	1j0tA00	1j5wB02	1j8uA00	1jadA00
1jekA00	1jeqA05	1jeyA04	1jfbA00	1jmuB02	1jmuB03	1jnrA03	1jqoA03	1jr8A00	1jvrA00
1jy2000	1k3eA01	1k6yA01	1k87A01	1k87A02	1k8kE00	1k8kG00	1k90C03	1kaeA03	1kblA02
1kblA05	1kmiZ01	1kmiZ02	1kn7A00	1kqfB03	1kqfC00	1kv4A00	1kyqA03	112pA00	115jA01
117mA02	118dA00	1191A00	1lnsA03	11s1A01	11shA02	1ltsC00	1lvkA03	1m15A01	1m56D00
1m6nA05	1m6yA02	1m7lA00	1m8oB00	1m93A00	1mc2A00	1mijA00	1miwA03	1mkmA02	1mn8D00
1mswD02	1mswD04	1mtyG01	1mtyG02	1musA01	1mw5A01	1mw9X02	1mxrA00	1mz9A00	1n31A02
1n62A02	1n81A00	1ng6A01	1ng6A02	1ngmB00	1nh2D01	1nhwC00	1nkdA00	1nu7D01	1nu7D02
1nxhA00	1ny9A00	100sA02	1oaiA00	1oaoC01	1ofcX03	1ohfC01	1oisA01	1oizB01	1oltA02
1on2A02	1or7C00	1orjD00	1orsC00	1ov9B00	1oxjA02	1p49A02	1peqA03	1pfiA00	1pjqA03
1pp9E01	1psrA00	1px5A02	1pyvA00	1pzqA01	1q08A00	1q16A10	1q16B03	1q5zA00	1q6hA01
1q7lB01	1qexA01	1qf8A01	1qgkB00	1qhdA02	1qsaA01	1qsaA02	1qu3A03	1qusA01	1r0dB00
1r5lA02	1r5sA01	1r71A01	1r89A01	1rf8B01	1rh6A00	1rrzA00	1rwhA01	1rykA00	1rzhM01
1s0pA01	1s2xA00	1s5jA05	1s7bA00	1s7zA01	1s9rA02	1s9uA00	1sauA02	1sd4A02	1sdiA00
1sedA00	1sf9A01	1sg7A00	1sigA00	1sknP00	1ss3A00	1sseB00	1sumB02	1svfA00	1svmA01
1svmA02	1szhA01	1szhA02	1t07A00	1t50A00	1t5oA01	1t6aA01	1t6uD00	1t77A02	1t9hA03
1tbaA00	1tbfA00	1td6A01	1td6A03	1tfeA02	1tgrA00	1tjlA00	1tkvA00	1tm9A00	1tr2A02
1tuzA00	1twfA05	1twfA06	1tx9A00	1u2zA01	1u57A00	1u7lA02	1u84A00	1u8vA01	1ufiC01
1ug7A00	1uiiA00	1uj8A00	1uptF00	1utgA00	1uujB00	1uvjA02	1v33A02	1v5eA04	1v74B00
1v9dA01	1v9dB00	1v9mA01	1v9mA02	1v9vA01	1vfiA00	1vibA00	1vk5A00	1vpcA00	1vpuA00
1vq8200	1vq8I00	1vq8P01	1vq8P02	1vq8P03	1vq8V00	1vq8W02	1vs5U01	1vsy300	1vt0M02
1vyiA00	1vykA00	1vzsA01	1w2yA00	1w36B02	1w36C06	1w36D01	1w59A01	1w9rA00	1wb9A03
1wleA01	1wmwB00	1wp9B03	1wpbB02	1wpbG01	1wrdA00	1wteB01	1wtjB01	1wu9B00	1wvfA04
1wxqA02	1wy5A02	1wy6A00	1wz2A05	1x3aA00	1x3zA03	1x6iB00	1x91A00	1xdpA01	1xfiA02
1xg0C00	1xhbA02	1x13C00	1x17A01	1xlyA00	1xmkA00	1xmxA03	1xn8A00	1xo0A02	1xouA00
1xq8A00	1xqoA02	1xszA02	1xtaA02	1xzpA02	1y02A01	1y0nA00	1y14A01	1y2mA03	1y6xA00
1y8aA02	1y9bA00	1y9bB02	1y9iA00	1yar001	1ye9A03	1yf2A02	1ygmA01	1ylmA00	1ymtA00
1yozA00	1yrtA03	1yu5X00	1ywmA02	1yx6A01	1z21A00	1z23A00	1z2zA03	1z3xA01	1z4hA01
1z5zA02	1z67A00	1z6mA02	1z6tA03	1z6tA05	1zboA02	1zbsA03	1zcdA00	1zeeA01	1zhxA02
1zkrB00	1zoqC00	1zroA02	1zs9A02	1ztdA00	1zx3A01	1zylA03	1zymA02	2a2bA00	2a2cA03
2a3dA00	2a5yB03	2a7kH02	2a7oA00	2adlA01	2ahmA00	2aibA00	2arhA02	2au3A04	2au5A00
2auaA02	2axcA02	2axqA03	2b1eA01	2b1eA03	2b39A07	2b3wA00	2b5uA02	2b6cA01	2b8iA00
2b9wA02	2bhyA03	2b12A00	2bnkA00	2c5uA02	2c9wA02	2ce7C03	2ch0A01	2ck3A03	2ck3D03
2ckxA00	2clyA00	2cs3A01	2cw8A02	2cw8A04	2cwoA01	2cwoA02	2cxnA03	2czsA01	2d11A00

```
2d2sA01 2d2sA02 2d48A00 2d4xA00 2d8dB00 2dbyA03 2debA01 2dgjA01 2dgyA02 2dlaA01
2doaA00 2dwkA00 2e1mB02 2e1mC02 2e31A01 2e87A01 2e8gA01 2e9xA01 2e9xB02 2e9xG00
2ebfX02 2efeA01 2elcA01 2endA00 2eo2A00 2eplX03 2erlA00 2es9A00 2eucA00 2ewfA02
2ex3B02 2f1kC02 2f23A01 2f48A03 2f4mB00 2f5jB00 2f6mD00 2f76X00 2f93B00 2fcwA00
2fh0A00 2fi0A00 2fiqA02 2fl4A01 2fm9A00 2fmlA01 2fsfB02 2fsiB04 2fyuF00 2g31A01
2g3vA00 2g5gX02 2g7oA00 2gaiA04 2gf4A00 2gfpA00 2ghjB02 2grrB00 2gumA02 2gytA01
2h5nC00 2h6fA00 2h7oA01 2h7oA02 2h88C01 2h88C02 2hd0A01 2hdwA02 2hgkA01 2hnhA03
2hoqA02 2hp0A01 2hvrA03 2i15A02 2i53A01 2i5uA00 2i6hA01 2i71A02 2iazA00 2ibpA01
2ibpA02 2ic6A00 2icwG01 2icwG02 2idbA03 2igpA00 2igsA00 2ii2A04 2ijqB00 2ijrA02
2ilrA00 2im9A03 2in3A02 2itaA01 2iw3A02 2iw5B00 2ixmA02 2ixsA01 2j0wA02 2j58A04
2j5yA00 2j7aC00 2j7nA02 2j8pA00 2j9wB00 2ja2A03 2ja2A04 2ja2A05 2jaeA03 2jbvA03
2jekA00 2jhpA03 2jiwA03 2jmsA01 2jnsA01 2jo7A00 2jpfA01 2jpnA00 2jqqA00 2jrmA00
2js3A01 2jspA01 2jugA01 2jv7A00 2jynA01 2k37A00 2k60A01 2k8oA00 2k9hA00 2k9pA00
2kbzA00 2kdcA00 2kebA00 2kicA00 2kinB01 2kjgA00 2kkeA00 2kkmA01 2klqA00 2kluA00
2kmuA00 2knjA00 2ko6A00 2koeA00 2kp6A00 2kr6A01 2krhA00 2ksdA00 2kseA00 2ksfA00
2kslA00 2ksnA01 2kvvA00 2kxeA00 2l1lB00 2l1nA00 2l3lA01 2l3nA00 2l5qA02 2l6oA02
217kA00 2laiA00 2lcuA01 2ld7B00 2lehA00 2lg1A01 2lg4A00 2lgqA00 2lhrA00 2lj2A00
21klA01 21kyA00 2110A00 21lvA00 21m0A01 21mkA00 21mzA00 21opA00 21orA00 21pbA00
2lq3A01 2lrdA00 2lrmA00 2lseA00 2lxeA01 2lyiA01 2lyyA00 2lzfA00 2lzrA00 2m3aA00
2m3eA00 2m4eA00 2m4hA00 2m5zA00 2m7aA00 2mabA00 2md0A00 2mgyA01 2mjfB00 2mjmA00
2mkzA01 2mphA01 2mrlA00 2mvtA00 2nn4A00 2nnuA01 2nq2A00 2nr5E00 2nsaA00 2nw8B00
2nxcA02 2nxpB00 2o36A01 2o36A02 2o57A01 2o5hA00 2o5iN05 2o6kB00 2o8sA01 2oa5A01
2oarC01 2oblA02 2oebA00 2oezB02 2okuA00 2om6A02 2oq1A02 2oqoA00 2ouxA01 2ov9A02
20x6D00 20x1A00 20y9A01 20y0A01 20zbB01 2p0nA00 2p0tA01 2p0wA03 2p1jA02 2p35A02
2p3yA02 2p62A02 2p9bA04 2p9xA00 2pbiA02 2pm7C00 2px0A01 2qcuA03 2qeeA02 2qfaC00
2qgmA03 2qguA02 2qklB00 2qkwA00 2qmaA01 2qmcC02 2qr4A01 2qr4A02 2qsbA00 2qtsA03
2qtsA04 2qtsD01 2qupA00 2qvwB05 2r18A01 2r4fD01 2r4gA01 2r4gA02 2r7rA02 2r7rA03
2r7rA05 2r7rA08 2r9gA02 2ra1A01 2ra1A02 2ra1A03 2rh3A00 2rhfA00 2rp5A00 2rreA00
2rt6A00 2uv8G01 2uv8G06 2uwmA01 2v1nA01 2v26A04 2v26A05 2v7kA01 2v7qI00 2vb1A00
2ve7C01 2vf1A04 2vf7A02 2vf7A03 2vgoC01 2vh3A00 2vj4A01 2vj4A02 2vj4A03 2vk9A03
2vk9A04 2vkjA00 2vqcA00 2vqeD01 2vqeT00 2vqgA00 2vs0A00 2vsgA02 2vugA04 2vxdA00
2vxzA02 2vzcB00 2w02B01 2w02B06 2w0gA00 2w4sA00 2w61A03 2w82A02 2w82A03 2w83C00
2w9yA00 2wadB03 2wb0X01 2wb7A03 2wbmA02 2wdtA01 2wf7A02 2wjnC02 2wl8C00 2wlvA00
2wscK00 2wssW01 2wviA00 2ww2A03 2wwxB00 2wxfA05 2x0qA04 2x1dA02 2x3mA00 2x49A03
2x98A02 2xauA04 2xepA03 2xf7A00 2xhiA02 2xmoA02 2xmxA01 2xquA01 2xqyA02 2xrhA00
2xs1A02 2xs1A03 2xusA00 2xv9A00 2y6xA00 2yb1A02 2yf4F00 2yfaB01 2ynmD04 2ynqA00
2ynzC01 2yqzA02 2yskA00 2yufA00 2z3qA00 2zcaB00 2zcmA00 2zi0B00 2zjsE00 2zm5A02
2zpaA04 2zshB00 2zuqA00 2zxiA03 2zxiA04 2zxqA06 2zy4A02 3a1yA00 3a2kA02 3a3cA03
3a4cA00 3a4mA02 3a98A02 3a9zA02 3aa0B01 3aekB03 3aj1B01 3ajfD00 3akjA02 3aqbA00
3ax2A00 3axjA01 3b0pA02 3b0xA01 3b0xA02 3b34A05 3b40A02 3b4qA00 3b4sA02 3b4sB01
3b5mC02 3b9wA00 3bc8A01 3bg1B03 3bg2A02 3bg2A03 3bg5B07 3bgeA01 3bh1A02 3bhwA00
3bnjA01 3bgkA02 3bgoA00 3buxB01 3bvxA02 3bzcA01 3bzcA02 3bzcA04 3c1qA00 3c1yA02
3c3dA02 3c4rA00 3c8zA02 3ca8A01 3cf6E01 3ci0K02 3ck6C02 3ckcA03 3ckdA01 3ckdA02
3clqA03 3cmnA01 3cnlA02 3cqxC00 3cr3A00 3crmA02 3crvA02 3csxA00 3cuqC01 3cveB00
```

```
3cx5C00 3cx5F00 3cx5I00 3cxbA03 3cxnB00 3d0wD00 3d1bB00 3d36C01 3d3bA00 3d8lA00
3dbyL00 3dfzA02 3dkxA02 3dorA01 3dp7A02 3dt5A00 3dteA01 3dteA02 3e2dA03 3ecsE01
3edvA01 3eg5B01 3eg5B03 3eh1A01 3ei3A04 3ei3B01 3er9B01 3ermB00 3errA01 3es5A02
3eslA01 3eslA02 3etvA01 3etvA02 3etzB00 3euhA02 3euhC02 3euhD01 3eujB00 3evyA00
3ez2A01 3eziA00 3f1iS00 3f2bA06 3f2bA08 3f4mA00 3f4sA02 3f75P00 3f7wA03 3f8tA01
3fajA00 3fbiD00 3fd9A01 3fd9B02 3fdqA01 3fedA03 3fgrA02 3fh3A00 3fhnA02 3fhnA03
3fhnA05 3fkeA01 3futA02 3fvvA02 3fwbB00 3fwnA03 3fxhA00 3g21A00 3g2bA00 3g36B00
3g5oA02 3g67A00 3g9kD02 3ggyA00 3gmfA02 3gmiA01 3gu3A02 3gw6A02 3gw7A00 3h0dA02
3h3aA02 3h3aA03 3h4cA02 3h90A01 3ha4B00 3hhdA05 3hhwA00 3hhwK01 3hhwK02 3hjlA03
3h16A02 3h18A04 3hr0A02 3i2kA02 3i4uA01 3i5pA03 3i9v104 3i9v201 3i9yA00 3iayA07
3ibpA01 3icxA02 3ieeA02 3if4A02 3ig5A03 3ig5A04 3igmA00 3iiiA02 3iisM00 3ikoC02
3ilxA02 3im1A01 3imiB02 3ip4C01 3iquA00 3ismC02 3itfA00 3iv6A02 3iylU02 3jrtA00
3jsbA01 3jszA03 3jvoA00 3k1zA02 3k40A01 3k4iC02 3k6tB00 3k8pC01 3k8pC02 3kalA03
3kevA02 3keyA01 3kfuG02 3kinB00 3kk4A01 3kmlA00 3kujA01 3kwlA02 3kwlA03 3l0iA02
310qA02 311nA02 314gC02 314gC03 31cnB00 31hrB00 31jbA00 3117A01 31mmC04 31ovA03
3lr2A01 3lxrF00 3m1mA03 3m4aA02 3m4wE01 3m66A00 3m6aA01 3m6jA01 3m6zA03 3m71A00
3m7gA02 3m8jA00 3m9lA02 3mayB00 3me5A01 3mhsB00 3mkqA03 3mmyB00 3mudA02 3mw6C00
3mzlB03 3n05A03 3n1eA02 3n2oA03 3n2oA04 3n40P01 3n50B02 3nb2A02 3nb2A04 3nbiA01
3nbxX03 3neuA02 3nfqB02 3nftA00 3nj2A00 3nkzA00 3nphB00 3nrwA00 3ns4A00 3nwsA02
3nzlA00 3o2rA00 3o3mB01 3o6xA02 3o79B00 3o7iA00 3o8mA01 3ojaA03 3okqA00 3o14A02
3omlA02 3omyA00 3onqA01 3onqA03 3opbA01 3oufB00 3oymA01 3p0bA02 3p2nB01 3p9aF00
3pieC02 3plnA02 3pmcA00 3pmgA02 3psfA01 3psfA05 3pubA01 3q23A08 3q9dB01 3qexA04
3qexA05 3qflA00 3qfsA02 3qilB00 3qyeB01 3r2pA02 3r6nA02 3r84A00 3rc3A01 3rc3A02
3rc3A05 3rfaA01 3rkiA02 3rkoA00 3rkoB02 3rkoF01 3rkoG00 3rlbA00 3rlfF04 3rq9A00
3rrkA02 3rrsA02 3rrwA02 3rv1A01 3rx6A00 3rznA01 3s13B01 3s6pD01 3sb1A02 3sbtB02
3seoA01 3shgB00 3sk9A00 3smvA02 3sqiA01 3sqnA02 3sqnA03 3swhA02 3sxmA00 3t38A01
3t92A00 3td7A02 3thgA00 3tjyA00 3tl4X01 3tl4X02 3tsoC00 3tu3B03 3tufA00 3u1cA00
3u4qA02 3u61A03 3u64A00 3u7qB03 3u9wA04 3ufbA01 3ugoA00 3ungC02 3ungC04 3uo3A02
3uo9C01 3ut4A00 3v3kD00 3v5uA02 3v5wA01 3v76A03 3vdpA01 3veaA01 3vhlA02 3vjfA00
3vldA01 3vldA02 3vtiA07 3vvmA02 3vw4A01 3vwnX02 3vywA01 3w54B00 3w7tA02 3wajA03
3wdcA00 3we0A03 3wfvA00 3wi3B00 3wkyB01 3wurA00 3x0uB01 3zc4A01 3zciA00 3zcoA00
3ze3B00 3zfiA00 3ziyA03 3zojA00 3zpxA02 3zr8X00 3ztaA00 3zykB02 4a15A02 4a15A03
4a1eO02 4a5uB00 4aaiA01 4acoA02 4adnA01 4adzA00 4ae4A00 4akgA10 4akgA13 4akgA14
4aklA02 4al0A00 4as2A02 4atgA00 4aumA02 4aybA04 4aybC02 4az6A02 4b0zA00 4b43A01
4b7hA03 4bgpA01 4bgpA02 4bjmC00 4bjqA00 4bllA01 4bllA02 4bpfA00 4bsxA00 4c1nA01
4c2mA08 4cayB00 4cfsA02 4ch7A01 4cihA00 4cs4A01 4cs9A00 4cyiA02 4dgwB01 4didB01
4djaA04 4dkcB00 4dlqA02 4dmvA01 4dq5B00 4dthA02 4du6E01 4dvzA02 4dx5C01 4e0pA02
4e40A00 4ebaG00 4ebjA02 4evxA00 4extA00 4eziA02 4f01A02 4f3fC00 4f55A01 4fasA01
4fasA02 4fcaA03 4fe3A02 4fhrB02 4fqgB03 4fqnC00 4fvmA07 4fwvA02 4fx5A03 4fz4A00
4fzlA01 4g2aA02 4g78A00 4gdoA00 4gmqA00 4gpkB01 4gxbA02 4gxtA02 4h3tA02 4h63H01
4h9dB00 4hfvA01 4hg2A02 4hi8A00 4hn9A02 4hr1A00 4hs2A00 4hstA02 4hy4B00 4i4tB03
4i8oA03 4iaoA01 4ihqA02 4ii2A05 4il6X00 4ip8A00 4ipeB04 4iqjM02 4irvA00 4izzB02
4izzB03 4j1vA00 4j32B00 4j8sA00 4ja3A02 4jk8A02 4jqfA01 4jquB00 4jrfA03 4jxhA01
4jzaA02 4jzaA03 4k35A03 4k51B00 4kbmB02 4kikA03 4kn7X01 4kp3C00 4kqkB01 4ks9A01
```

```
4kt6A01 4kt6B00 4l57A02 4l74A02 4lerA03 4lgdB02 4lgyA02 4lixA02 4lrvF00 4lupA00
4m0wA02 4m70B00 4mewA01 4mewA02 4mf5A02 4n7wA00 4na1B02 4nc6A02 4nc7A00 4ne3B01
4nomA02 4nooB00 4npdA00 4nqwB00 4nurA02 4nuuA02 4o8sA02 4ofzA01 4ogqB02 4ogqC03
4ohfA03 4onrA00 4owfA00 4p02B05 4p09A00 4p0pB02 4p3aA00 4p3fA00 4phqA00 4phzA02
4phzB00 4phzG00 4pw8F02 4q68A01 4qozC00 4qpkA01 4qreA03 4ragA02 4rgdA00 4rr2B00
4rwuA00 4s12A02 4tq1A03 4tx5B00 4u5hA00 4u7bA01 4ud4A01 4udxX01 4uelA02 4v3iA00
4w4kB00 4w8pA01 4w8pA02 4wbyA02 4wfoA05 4xpxA00 4xvvA00 4y97D00 4yonA01 4z3xA03
4z49A02 4z8lB00 4z9hB00 4zdsB00 4zeyA00 4zi3D00 4zldA00 4zpcA03 4zzxA01 5a0yA03
5ajiB01 5azpB01 5b1aB01 5b1aC02 5b1aD00 5b1aE00 5b1aH00 5b66C02 5b66H01 5bseA02
5c05A01 5c5aA00 5c5oA03 5cklA00 5c18A00 5cqeB01 5cqgA03 5cqgA05 5decA02 5dm6200
5eehA02 5ep2A02 5f2kB01 5fbfA00 5figA00 5gmzA00 5grqA00 5gudB01 5hayA02 5i34A02
5ig6A00 5ii8A00 5j71A01 5jajA03 5jbxA02 5khtA00 5l44A01 5lp0A00 5m33B00 5mk2B00
5mtvA01 5nkfA02 5nrmB00 5ok4A02 5osiK00 5oswA03 5oy0000 5oy0600 5svhA00 5taoA02
5tt5A01 5tuxA01 5tzdB00 5ui5I01 5uqmA03 5uukA00 5v37A03 5v37A04 5vfbA03 5w6yA00
5wkrA02 5xnsC00 5xxuG02 5xzgA01 5y5s200 5yceA00 5yghA00 5yrvC02 5ysnA02 5ysnB01
5z0fA00 5zw7A03 6aeqA00 6am3A00 6b4eA00 6cgvM01 6d55B01 6d55B02 6dcjA02 6dhqA01
6e3aA01 6e5yA03 6ekzA00 6eniA00 6faiI03 6g1iA00 6g1pB00 6gfxC02 6ghdG00 6hx1A03
6hzwA02 6i5aA00 6ibeA02 6iumA03 6m9mA01 6m9mA02 6mx3A01 6n1mA01 6neqN01 6nsjA00
6q4rA04 6q52A04 1a1xA00 1a3qA01 1ayoA00 1b12A02 1bg1A02 1bxoA02 1c4qA00 1c5eA00
1cq3A00 1dgwX00 1dqcA00 1e2wA01 1e8rA00 1e16A02 1ep3B03 1euwA00 1ezgA00 1f00I02
1f15B00 1f35A00 1f86A00 1feuA02 1fjrA01 1fjrA02 1g3pA01 1g6eA00 1g8kC01 1gk9B02
1gkuB01 1gkuB07 1gp0A00 1h4gB00 1h5wB02 1h6fA00 1h6wA01 1h6wA02 1h8pA02 1hyoA01
1ib8A02 1im3D00 1io1A02 1io1A03 1irxA02 1jb3A00 1jb7B00 1jbiA00 1jjdA00 1jmuB04
1js8B02 1jv1B02 1k0hA00 1k32A01 1k3iA02 1k4zA00 1kg1A02 1kmoA01 1kzqA02 1lmlA03
1lmlA04 1lpbA00 1lshA01 1lshA03 1lshA04 1lshB00 1lxmA04 1m8nB00 1m9sA03 1mbyA00
1mkcA00 1mkfA01 1mkfA02 1mknA00 1mw9X03 1n7vA02 1n7zA01 1n7zA02 1n9pA00 1nc7A00
1njhA00 1nltA02 1nnxA00 1np6A02 1nycA00 1o70A01 1o75A02 1o75A03 1o75A04 1odhA01
1ofdA04 1oisA02 1ok0A00 1opoA02 1oruA00 1osyB00 1ou8A00 1ow1A00 1pbyA02 1pinA01
1pm4A00 1pv5A00 1qd5A00 1qexA02 1qexA03 1qhdA01 1qwyA01 1r4xA01 1r6vA01 1r8oB01
1ra0A01 1rcqA01 1rgxA02 1rlhA01 1ro2A03 1rocA00 1rwhA02 1rwhA03 1s1dA00 1s4cC00
1s7mA03 1sf9A02 1sg5A01 1so9A00 1svbA01 1t60D00 1ti2A01 1tlyA00 1tulA00 1twfB06
1twfB07 1twfL00 1uhvA01 1uoyA01 1ut7B01 1uunA01 1uunA02 1v7wA02 1vmoA00 1vq8Q00
1vq8U00 1vq8Z00 1vw4M01 1vwxZ00 1vziA01 1w5rA02 1w8uA00 1w99A03 1whiA00 1wjxA00
1wktA00 1wlgA02 1wruA01 1wthA01 1wthD03 1wwyA00 1x0cA01 1x54A01 1x9pA01 1xakA00
1xf1A03 1xhhA00 1xo8A00 1xvsA00 1y43B00 1y71A00 1ya5T01 1yduA01 1ye9A02 1yg9A01
1yhpA02 1yi9A01 1yq5A00 1yu0A01 1yu0A02 1yueA02 1yvuA02 1ywmA01 1z0sA02 1z47A02
1zc1A01 1zhxA03 1zldA00 1zruC01 1zxuA00 2a6hC04 2a7yA00 2ae0X02 2aegA01 2ag4A00
2axwA01 2aydA01 2b9kA00 2bcoA02 2bdrA00 2bmoA02 2bonA02 2bt9C01 2bvbA00 2bw4A01
2c1lA02 2c9oB02 2ck3D01 2covG00 2cr8A01 2d42A01 2d5bA02 2d9rA00 2de6A02 2df7A02
2dpfA00 2dsxA00 2dyiA01 2dyiA02 2e12A00 2e3hA00 2e4uA03 2e5yA01 2e6fA02 2e7zA01
2e9hA02 2eabB01 2ed6A01 2f01B00 2f0cA02 2f1cX00 2f5tX02 2f6eA00 2fhdA02 2fj8A01
2f17A00 2fsdA00 2g50F03 2g5dA03 2giaB00 2gk6A02 2gujA01 2gumB01 2h6oA01 2h6oA02
2h6oA03 2hb0A01 2hbpA00 2hd0A02 2hjeA02 2hmaA02 2hnuA00 2hoxA01 2hsiA01 2hu9A01
2hzmA02 2i46A00 2i7cA01 2in5A00 2iumA00 2iw3A05 2j8bA00 2j8gA03 2j8kA01 2j98A01
```

```
2jjqA03 2jl6101 2jmbA00 2jn4A00 2jn9A01 2jneA00 2joxA00 2jr3A00 2jsnA00 2jubA02
2jvuA00 2jyeA01 2k49A00 2k5dA01 2kcaA00 2kcpA01 2kieA00 2kssA01 2kxyA01 2kzbA00
210zA00 211tA00 215qA01 216oA01 216uA00 21g7A00 21gnA00 21iyA00 21r4A00 21s0101
21v1A01 21w3A00 21w6A00 2m3xC02 2m41A00 2m5sA00 2m6oA00 2m9uA00 2mcaA00 2mcmA00
2mctA00 2mhdA00 2mhgA00 2mm0A00 2nnuA02 2nv4A00 2o9sA00 2odxA00 2oezA01 2oizA01
2oj5D00 2opcA00 2ox7A01 2ox7A02 2p3yA03 2p3yA04 2p84A01 2pa8D02 2pbdA02 2pieA01
2pn5A01 2pp6A02 2pw8I00 2q4zA02 2q6kA02 2qcpX01 2qf4A01 2qf4A02 2qkdA01 2qkdA02
2qngA01 2qq9A03 2qqpA03 2qsfA02 2qtsA02 2qtwB02 2qzbA00 2r5oA01 2ra1A05 2ra9A02
2rdkA00 2rdqA00 2rprA00 2rrfA00 2uv8G09 2v05A01 2v0cA03 2v3iA00 2v8iA02 2vbuA01
2vf1A02 2vhjA02 2vldA01 2vrsA02 2vrsA03 2vveA02 2vvfA01 2w02B02 2w02B04 2w1jA00
2w4yA00 2wb7A02 2wkdA00 2wn9D00 2wtpA00 2wy3B00 2wzpP01 2wzpP03 2wzpP04 2wzpR01
2x12A01 2x2zB03 2x4jA01 2x8sA02 2xc1A01 2xdwA02 2xfdA00 2xtsA02 2xvoB00 2xwxA03
2y3vD00 2y4yA00 2y5pA00 2y7lA02 2y8nB01 2yfoA01 2ygoA01 2yjlA00 2ylbC00 2ymoA02
2ymsB00 2yo3A02 2yq2A01 2yq2A02 2z0tB00 2z14A00 2z2mD02 2z3qD01 2zahA02 2zaiA04
2zf8A01 2ztbA02 2ztbA03 2zuoA08 2zwsA02 2zx2A02 2zxeB02 2zxiD02 2zxrA01 2zyrA02
2zyrB03 2zzeA03 3a54A01 3a57A00 3a5pA00 3aehA00 3aibB01 3aiiA02 3aiiA03 3ar4A01
3askA02 3b08E00 3be3A00 3bh4A02 3bs1A00 3bt4A00 3bvxA04 3bvxA05 3bwzA00 3bywB00
3c2qA01 3c5xC00 3c7xA00 3c8iA00 3c9aA02 3c9aA03 3ci0J02 3d79A02 3d9xA02 3dclA01
3df7A03 3dohA01 3dsoA00 3dtdD00 3duzA02 3dzmB00 3e0jA02 3e1sA04 3e3xA03 3e7jA03
3ecqA01 3eh1A03 3eo5A01 3es1A01 3esmA00 3exmA01 3f3bA00 3f3fD01 3f59D00 3f6kA02
3f7lA00 3fbqA01 3fbqA02 3fdjA02 3fgrA01 3fidA00 3fkeA02 3fmgA02 3fo8D02 3fqmA01
3fqmA02 3fssA01 3fvqA02 3fvqA03 3g1jA00 3g74C00 3gbwA00 3gefA00 3ghmA03 3girA04
3glaA00 3gnfB04 3gnfB06 3go5A01 3h99A02 3hagA02 3hhtB02 3hieB01 3hlkA01 3holA03
3hrzA03 3hrzB01 3hrzC01 3hxlA02 3i57A02 3iagC01 3if4A01 3ii2A00 3ioxA02 3ipfA01
3ix0A02 3j26N01 3j4uH00 3jqoA01 3jqoB00 3ju4A03 3jybA00 3k2zA02 3k59A01 3k6oA01
3kbgA02 3kffA00 3kihC01 3kihD00 3ku3A01 3kwdA00 3kxtA00 3l81A01 3lazA01 3ld7A00
3lyrA00 3lzqA00 3m4yA01 3m7aA01 3m7oA00 3mcbA00 3mqgA02 3mtvA01 3mudA01 3mx7A00
3mxnA01 3mzfA02 3mzlB01 3n40P02 3n40P03 3n40P04 3n5bB01 3nbcA00 3nbiA02 3nbxX04
3nisA01 3njaA02 3nk4A02 3nk4B01 3nkgA00 3nrlA00 3nswA00 3obhA00 3oblA00 3oe3C00
3og2A02 3og2A03 3oipA01 3on9A00 3p02A02 3p24A01 3p4gD00 3p8aA02 3pfgA02 3pieC05
3pieC09 3pojB00 3pqhA01 3pqhA02 3pquA01 3qc5X01 3qdrB00 3qjoA03 3qrlA00 3qzmA00
3rbyA01 3rbyA02 3rfzB04 3rj2X00 3rkgA01 3rlfF03 3rmqA01 3rr6A01 3rwnB00 3rwxA02
3s6pA03 3s9zA02 3sbtB01 3sovA02 3t4nB01 3tewA02 3tewA04 3thtA02 3tixB01 3towA00
3ttvA01 3u28C00 3u2gA01 3u2gA02 3u4kA00 3u6xS00 3u9wA01 3uafA00 3ujzA03 3upuA03
3v0dA02 3vhxF00 3vkiA02 3vsmA02 3vsmA03 3vtnA01 3vwoA02 3vypB01 3w1eA03 3w5hA01
3w9eC00 3wajA04 3wdhA01 3wkyB03 3woeB00 3wqcA01 3wttB00 3wvtA01 3wx7A02 3x2mA00
3zbdA00 3zc4F02 3zfpA02 3zghA00 3zjaA01 3zn4A00 3zn6A01 3zn6A02 3zpeA00 3zpnC00
3zucA00 3zx7A01 3zxaC02 3zy7A00 3zzsA00 4a02A00 4a0tA03 4a2vA00 4a7kA02 4a94C00
4adiA01 4afmA00 4apmA03 4apxB01 4aq1A03 4aq1A04 4aq1A05 4aqzA00 4arcA04 4aybA06
4b1mA00 4b3fX02 4b9gA00 4bfoA00 4bhuA00 4binA01 4bjjB00 4bxmB00 4c00A04 4c08A02
4c9rD00 4cc0A01 4cc0B02 4ckbA03 4csqA00 4cv7A00 4d8mA03 4da2A01 4deqA02 4dixA01
4dixA02 4dlqA03 4dmiA02 4dnyA00 4dt4A02 4dt5A00 4e5xG00 4eaeA00 4egdA00 4egvA02
4ei0A01 4eirA00 4en6B02 4epsA02 4eqaC00 4eqpA00 4es8B01 4f01B01 4f5cF00 4f9aB01
4fcaA01 4fchA01 4fchA02 4fdwA01 4fe9A01 4fgmA01 4fibA02 4fnvA02 4fo0A02 4fp5D00
```

```
4fx5A01 4fyyB02 4g1gA02 4g1lA01 4g2aA01 4g3nA00 4g7xA00 4gipD02 4gipD03 4gmuA02
4gouA02 4gpvA02 4gqzD00 4gucA00 4gv5A00 4gy7A03 4h14A00 4h3wA01 4h4nA00 4h6cB00
4hceA00 4hfsA00 4hgzA02 4hi6C00 4hi8B00 4hj1A01 4hj1C03 4hkjD00 4hn7A00 4hscX04
4hspA00 4hu2A01 4i1kA00 4iauA02 4iefA00 4ii2A03 4ildA03 4indA01 4indA02 4indA03
4innA00 4it6B00 4jadA01 4jcwA02 4jdeA01 4jdnC00 4jg9A00 4jj0B00 4jw0A00 4k15B00
4k7jA02 4kbxA01 4kh8A02 4khbC00 4khbD02 4kk7A03 4kkrA02 4krwA00 4ku0D00 4l3fA02
4lbaA01 4ld1A00 4ldvA03 4le3C00 4le7A01 4lo6B03 4luqC00 4m0nA01 4m0wA03 4m4pA02
4m8rA01 4mbyH00 4mqdA00 4mtmA01 4mveA00 4mzgB00 4mziA00 4n1iA00 4n6qA00 4nbmA00
4nohA02 4nx9A02 4nzrM02 4o4oA00 4o65A00 4ohxA03 4ohyA01 4oj5A02 4ojdH01 4ojdH03
4opwB00 4oq1A01 4oq8A00 4osnA00 4ousA00 4p5nA00 4phzA03 4pj2A00 4pn6A00 4q63A00
4q68A02 4qa8A00 4qclA01 4qi3A00 4qp5A00 4qxaB00 4r4xA02 4r84A01 4rdbA01 4rlzA02
4uhvA01 4uhvA04 4uybA02 4v33A01 4w6yA00 4wdcA00 4weeA01 4wfoA01 4whiA00 4whsD00
4wk0B02 4wkzA01 4wz8B02 4x5pA00 4xjwA03 4xotA03 4yn3A03 4ysiA00 4yx1A00 4z3gA00
4z4dA02 4z8jA00 4zboC00 4zcnA00 4zgfA00 4zzfA02 5a67A00 5aq0B00 5avdA02 5azpA02
5b1aF00 5cybA00 5d7uA00 5d7wA01 5dhdA00 5dm6U00 5dmdA00 5e62A01 5ffgA02 5fo8B03
5fvnA00 5g38A00 5guaA00 5gv0A00 5h3xA01 5hqhA00 5i2mA01 5i2mA03 5i8gA03 5ihwA01
5ihwA02 5itmA00 5iucA00 5ixgA00 5k8sB00 5kvfE00 5kycB02 5lndB00 5lzhA00 5m04A01
5nqzA02 5nqzB01 5o95D01 5tipA02 5u3aA02 5u47A01 5umsA01 5uv8A01 5v1yB00 5vqfD01
5wkwA02 5x91A00 5xogM00 5ycqA00 5yj6A02 5ysnA01 5zw7A02 6bogA02 6c6zA02 6e41A00
6f2mA02 6fgcA03 6fgdA04 6fjnA00 6fmeA03 6gecA00 6ha4A00 6hoyA02 6itaA00 6iw3A00
6myiB00 6nfrA00 6q4rA03 16pkA01 1a73A00 1a87A01 1a9xB01 1aolA00 1b33N01 1bbgA00
1bm8A00 1bmlC03 1bplA01 1bxyA00 1byiA00 1c96A01 1c96A02 1ccwA00 1ccwB02 1chdA00
1cksB00 1c18A00 1co4A00 1cqmA00 1cvrA01 1d0qA00 1d4uA00 1d5tA02 1dd9A01 1dfmB00
1divA02 1dj0A01 1dj0A02 1dq3A02 1ds1A00 1dtdB00 1dw9A02 1dy5A00 1dzfA01 1dzfA02
1e2tA02 1e59A00 1e7lA01 1eiwA00 1e16A03 1eu1A02 1eu1A03 1euvA02 1ewqB01 1ezwA00
1f08B00 1f0xA01 1f0xA04 1f32A01 1f3mA00 1f46B00 1f9vA00 1fd3A00 1fiuA00 1floA01
1fm0E00 1fn9A01 1fn9A02 1fo8A02 1ftrA02 1g2rA00 1g3pA02 1g8kA01 1gaxA04 1gccA00
1gd8A00 1ghhA00 1gk8I00 1gkuB04 1gqeA02 1gqiA01 1gqiA03 1gxlA02 1h4xA00 1h5wB03
1h6wA03 1h8eG02 1hdoA00 1hf2A01 1hi9A01 1hi9A02 1hq0A00 1hqkA00 1hufA00 1i4jA00
1ib8A01 1igdA00 1ii7B02 1ikpA02 1iq4A00 1iq8A02 1iq8A03 1iqoA00 1iqzA00 1itxA02
liuqA02 lix9A02 lj0pA00 lj24A00 lj27A00 lj3aA00 lj5yA02 lj6rA00 lj7xA01 lj8bA00
1j98A00 1jb0D00 1jetA02 1jetA03 1jg5A00 1jljA00 1jmuB01 1jo0A00 1ju2A02 1k0rA01
1k1xB01 1k20A02 1k4iA00 1k4tA03 1k5nA01 1k7cA00 1k8bA00 1k8kD01 1kafA00 1kblA03
1kgdA02 1kjqB02 1kjqB03 1kn6A00 1ko7B01 1kp8A02 1kptA00 1kvdB00 1kwmA01 110wA03
11fpA03 11mlA01 11mlA02 11qtB02 11u9A01 1m15A02 1m5q102 1mg7A01 1muwA00 1mw9X01
1n0eA00 1n0uA03 1n2mC00 1n6zA00 1n91A00 1nd9A00 1neiA00 1nijA02 1nkiA00 1nm8A02
1nnvA01 1nr3A00 1nt2B01 1nu0A00 1nwzA00 1nxiA00 1nxuB03 1o0sA03 1o75A01 1o7jA02
108rA00 1098A01 109iA02 10aoC03 10aoC04 10aoD05 10c7A00 10dhA02 10hgA01 10i2A01
10i7A02 10kgA03 10msA00 10o0A00 1oz9A00 1p1hB01 1p6oA00 1p9gA00 1pbuA00 1pg6A00
1pj5A03 1pn0A03 1poiA02 1pp0B00 1pz4A00 1pzwA00 1q16A09 1q11A00 1q60A00 1q6zA02
1q7zA01 1q9uA00 1qd1A01 1qd1B02 1qhhD01 1qnaA01 1qqrB00 1qs1A01 1qtnB00 1qu3A05
1qv9A01 1qw2A00 1r0mA01 1r0rI00 1r6xA01 1r7lA00 1r89A03 1r89A04 1regX00 1rifA01
1rk6A03 1rkiA01 1rkuA02 1rl6A02 1ro2A01 1ro2A02 1ro7C00 1rozB00 1rtqA00 1rv9A00
1rylA00 1rzhH02 1s61A02 1sauA01 1seiA01 1seiA02 1sgoA01 1sr8A02 1ss6A01 1stzA03
```

```
1sziA01 1szwA01 1szwA02 1t23A00 1t6aA02 1t8sA01 1td6A02 1tdjA03 1tf5A02 1tfeA01
1tifA00 1tigA00 1tt8A00 1twfA04 1twfA09 1twfB05 1twfB08 1twfF00 1u02A02 1u07B00
1u0sA00 1u3eM01 1u6zA04 1u7iA01 1u7iA02 1u7lA01 1ua4A02 1ucdA00 1ucsA00 1ud9A00
1udxA03 1ugiD00 1uglA00 1utaA00 1uv7A00 1uvjA03 1uwkA02 1uwkB01 1uzkA02 1v0uA01
1v4pA02 1v5iB00 1v5rA00 1v5vA02 1v74A00 1v7zA00 1v8cA02 1v8dC00 1vajA01 1vajA02
1vbkA01 1vbkA02 1vbwA00 1vclA03 1vk8A00 1vq8S00 1vq8B03 1vq8C00 1vq8H00 1vq8L02
1vq8M00 1vq8X00 1vqqA01 1vqqA03 1vr4C00 1vr9A02 1vsrA00 1vw3C02 1vwxr00 1vwxU00
1vx2I02 1vz0A01 1vzyA01 1w2wB00 1w36C01 1w5rA01 1w94A00 1w96A02 1wb9A02 1wcwA01
1wd5A02 1wddA01 1wddA02 1wfxA02 1whzA00 1wiwA01 1wjvA01 1wkvA01 1wn2A00 1wn9A00
1wpnA00 1wteA02 1wthA02 1wthD02 1wthD04 1wtjA02 1wu7A02 1wv8A00 1wvfA03 1wvqC00
1x1oA01 1x3lA01 1x3lA02 1x4sA00 1x6mA00 1x74A05 1x7dB01 1x7iA00 1x9tA02 1x9yA01
1xbiA00 1xdnA01 1xdnA02 1xdpA02 1xeeA01 1xg0B00 1xk7A01 1xppD00 1xqbA02 1xszA03
1y0kA00 1y56A01 1y5iA02 1y60A00 1y6uA01 1y6zA01 1y7pB02 1yd0A00 1ygtA01 1yj7B01
1ylxA00 1yr1A00 1yrtA01 1yrtA02 1yuaA01 1yueA03 1ywyA00 1z0sA01 1z2nX01 1z2nX03
1z2zA02 1z8gA01 1zatA01 1zelA01 1zhsA01 1zhxA04 1zjcA01 1zl0B01 1zpsA01 1zr6A01
1zylA01 1zzkA00 2a1kA00 2a1sC02 2a1vA00 2a2pA01 2a50C00 2a6hC02 2a6hD09 2abyA00
2aebB00 2aegA02 2aeuA01 2ahmH02 2arzA02 2auwA01 2ayaA00 2ayxA01 2b5uA03 2b97A00
2b9wA03 2bbhA01 2bh1X00 2bkyA00 2blnA01 2blnA02 2bmoA01 2bn8A00 2bs2A04 2bw2A01
2bw2A02 2c0nA00 2c1iA01 2c1iA02 2c42A03 2carB00 2cjaA01 2cjsC01 2cveA01 2cviA01
2cw9A00 2cx0A01 2cxaA01 2cxaA02 2cxiA01 2cxiA02 2cxnA02 2cyjA00 2czrA01 2czrA02
2czvC01 2d0oA02 2d0oA03 2d1cA02 2d42A02 2d46A00 2d56A00 2d74B01 2d7eA01 2dbsA00
2de3A02 2dgmC03 2dkoA00 2dlaA02 2dlbA00 2dm9A00 2dsmA00 2dstA00 2dulA02 2dxaA00
2dy0B00 2dy1A03 2e0zA01 2e1mA03 2e1mA04 2e1mC01 2e29A01 2e2fA00 2e52B01 2e7vA01
2e7zA02 2e9xB01 2e9xD02 2ebeA00 2ebfX04 2ecsA00 2efvA00 2eiyB02 2ekdA00 2elcA02
2eplX01 2etxA01 2ew0A00 2ewfA03 2ex2A02 2f40A00 2f4qA01 2f5gA00 2f6uA00 2faoA01
2fb6A00 2fd4A00 2ffgA00 2ffmA00 2fgyA03 2fhzA00 2fhzB00 2fipA00 2fmaA00 2fphX01
2fpnA01 2fpnA02 2frxA02 2fvyA01 2fz0A00 2fz4A01 2g3wA00 2g7hA01 2g7jA00 2gagC02
2gagD00 2gefA02 2gfqA02 2gfqB01 2gg2A00 2gjhA00 2gjvA00 2gk4B00 2gkpA00 2gmhA02
2gn4A02 2gnxA02 2gp4A03 2gq0B02 2gqcA01 2griA01 2gsoA02 2gtiA01 2gukA00 2h1vA01
2h7aA01 2hafA02 2hbaA00 2hc5A01 2hd9A00 2hdiB00 2hekA02 2hfqA00 2hg6A00 2hg7A00
2hh8A00 2hiyA02 2hiyB01 2hj1A00 2hjeA01 2hjjA00 2hjqA01 2hngA00 2hp0A02 2hpuA01
2hpuA02 2hq4A00 2hqsA01 2hw4A01 2hy7A01 2hzmG01 2i06A01 2i06A02 2i1sA00 2i5vO02
2i71A01 2i9iA00 2i9xA00 2ia1A01 2iafA00 2ih2A02 2iihA00 2iruA02 2it2B00 2iutA01
2ixsA02 2ixtA00 2j0aA00 2j4mA02 2j58A01 2j58A03 2j6bA00 2j7qA00 2j9lA02 2ja2A02
2jaeA02 2jcbB00 2jfrA00 2jh3A03 2jh3A04 2jisA01 2jmkA00 2jobA00 2joeA01 2joiA00
2jovA01 2jr1A01 2jroA01 2jubA01 2jvnA00 2jwgA00 2jwhA00 2jwkA00 2jyaA00 2jz7A00
2k2wA00 2k35A00 2k3dA00 2k4nA00 2k4vA00 2k5cA00 2k87A00 2kafA00 2kc5A01 2kdpA00
2kdxA00 2kgsA01 2kgyA00 2kjxA01 2kk4A00 2kkxA00 2kl5A00 2km1A00 2konA00 2kouA00
2krxA01 2kswA01 2kt9A01 2kvtA00 2kx2A00 2kx7A00 2l1aA00 2l25A00 2l48A00 2l6mA00
216qA00 218eA00 218kA00 219dA00 21c0A00 21epA00 21ezA00 21f0A02 21jwA00 21lzA01
2ln3A00 2lnaA00 2lsmA00 2lu1A00 2luyA01 2lyxA00 2lz0A00 2m1sA01 2m3kA00 2m4iA01
2m5yA01 2m7oA00 2mc5A00 2mcfA00 2mekA00 2memA00 2mheA00 2mj6A00 2mmpA00 2mn5A00
2mqdA00 2nsfA02 2ntkB00 2nzwA01 2nzxA02 2o90A00 2o9uX00 2oa9B02 2ob3A00 2ob9A00
2od0A00 2odiA01 2odkA00 2ogfA00 2olvA01 2opeA00 2orwB02 2os0A00 2outA01 2p09A00
```

```
2p0wA01 2p4bB02 2p62A01 2p9bA02 2p9bA03 2pfcA00 2pffB05 2phnA01 2phnA02 2pifA01
2pifA02 2pn0A02 2pofA00 2psbA00 2pwwA00 2py5A03 2q07A01 2q18X01 2q5cA02 2q6kA01
2q7dB01 2q82A00 2qa1A02 2qgmA01 2qgmA02 2qgqB01 2qhqB00 2qmuC00 2qnuA00 2qq4I00
2qsdB02 2qsfA03 2qsfA04 2qtfA01 2qudA00 2qyaA01 2qyfB00 2qyzA01 2qziA00 2rocA03
2r31A01 2r41D00 2r4fA02 2r6zA01 2r7rA04 2r7rA07 2ra9A01 2rbgA00 2rbkA01 2rbkA02
2rinA02 2rngA01 2rrlA01 2rrnA01 2rsxA00 2sakA00 2sicI00 2uv8A01 2uv8A06 2uv8G03
2uv8G07 2uv8G12 2ux9C00 2v0eA00 2v3aA03 2v4bA02 2v89A01 2v8iA03 2va0A00 2vdwB02
2ve7C02 2vfrA02 2vfrA03 2vfrA04 2vobB03 2vouA02 2vpzA04 2vsgA01 2vugA05 2vwsA00
2vxnA00 2w02B07 2w2gA02 2w2gB01 2w2sA00 2w56B00 2w5qA01 2w6kA00 2w7aB00 2w82A01
2w8mA00 2wb0X02 2wb6A00 2wbmA01 2wbnA00 2wcwB00 2wdcA03 2wdsA00 2wdtC02 2wgoA00
2wj9B00 2wmmA02 2wnfA00 2wnpF01 2wqkA00 2wshB00 2wteA01 2ww2A02 2wyhB01 2wyoC01
2wzoA01 2wzpR02 2wzpR03 2x0dA01 2x0qA01 2x3dF01 2x3gA00 2x3lA01 2x49A02 2x49A04
2x5cA01 2x5hA00 2x5oA03 2xanA01 2xciC01 2xepB01 2xfvA00 2xhiA01 2xi5A00 2xlkB00
2xqyA01 2xtsA01 2xu3A00 2xu8A00 2xw6A00 2xxlA01 2xxpA02 2xzn800 2y2mA03 2y2pA01
2y3mA02 2y78A00 2y8yA01 2y8yA02 2ychA02 2yh5A00 2yilA02 2yimA02 2yjgA01 2yjgA02
2ykfA01 2ykoA03 2yqpA00 2yreA01 2yt4A01 2yvsA02 2yweA05 2yx1A01 2z0jH00 2z0rC00
2z51A01 2z5bA00 2z6rA02 2z6rB01 2z84A00 2zdjA00 2zejA01 2zixB01 2zk9X00 2zktA02
2zpaA01 2zt5A02 2ztbA01 2zueA01 2zw2A00 2zxpA02 2zxrA04 3a1pB00 3a2eA00 3a2kA03
3a2vD02 3a9lA00 3a9sA01 3a9sA02 3a9sA03 3aa0A01 3aa0B02 3adyA00 3agkA01 3agnA00
3aj1A02 3ajdA01 3ajeA02 3ajvA01 3akjA01 3aqoA01 3aqoA02 3ayjA02 3b0gA01 3b0xA04
3b21A00 3b34A02 3bbbC00 3bcyA00 3bf0A02 3bh1A01 3bh1A03 3bidA01 3b14A02 3b19A01
3b19B02 3bm3A00 3bmxA02 3bq9A01 3bqwA02 3bsuA00 3bt3A01 3bu2A02 3bwhA01 3c19A01
3c19A02 3c2qA02 3c4aA02 3c6aA00 3c6fA02 3c8yA01 3c9qA00 3canA00 3ccdA00 3cetB02
3ci0J01 3cimC00 3clqA02 3clqA04 3covA02 3ct6A00 3ctzA02 3cvzC01 3cwcA02 3cwcB01
3cwxA00 3cxbA01 3cxbA02 3cypB00 3d03A01 3d03A02 3d1pA00 3d2qD00 3d3bJ00 3d7jA00
3dd6A01 3df6B00 3df7A01 3dgpA00 3dgpB00 3dk9A03 3dktA01 3dkxA01 3dnjA00 3do9A01
3dplC02 3drxB03 3dteA03 3dupA02 3e0jB00 3e0jC01 3e0rB02 3e1tA02 3e2dA01 3e8tA00
3eipA00 3ejbB01 3ekiA01 3ekiA02 3eoiA00 3ep6B01 3er9B03 3essA00 3eyeA00 3f0dA00
3f2bA04 3f6gA01 3f6kA03 3fanA03 3fedA02 3ffvA00 3fgrB00 3fgxA00 3fjuB00 3floA02
3fmgA01 3fn2A00 3fndA02 3foaB01 3fpnB00 3frnA01 3fuyA00 3fy6D01 3fylA00 3g2oA01
3g4nA01 3g4nA02 3g8qA02 3g91A00 3g98A00 3gd0A02 3ge3C00 3ge3E00 3giuA00 3gk7A02
3gmxA00 3go9A02 3gocA00 3goeA00 3goxA02 3gw6A03 3gwiA00 3gywA02 3h09A03 3h0dA01
3h1dA01 3h1dA02 3h1dA03 3h2tA01 3h35C00 3h5jA00 3h7hA01 3h7hB00 3hbmA01 3hg9A01
3hgtA00 3hhtA00 3hi2B00 3hidA01 3hj4A02 3hjeA02 3hjhA01 3hjhA03 3hl6A01 3hl8A02
3ho6B00 3hshE00 3hxlA01 3hxlA03 3hxlA04 3hxlA05 3hz7A00 3i0wA01 3i57A01 3i9v102
3i9v103 3i9v600 3i9v700 3i9v900 3icjA03 3iekA02 3ifuA02 3ig5A02 3ihmA02 3im9A01
3imoC00 3iohA00 3ip0A00 3ipjA01 3it4B01 3it4D02 3iwcB00 3iwcC00 3iwgA01 3ix3A00
3ixlA00 3iylW01 3iylW02 3iylW03 3jsyA01 3jsyA02 3jtnB00 3ju4A01 3jv1A00 3jyoA01
3k11A01 3k11A02 3k1tA02 3k2yA00 3k3vA00 3k4iC01 3k59A02 3k63A01 3k6mD01 3k7iB00
3k85A00 3k8wA02 3ka7A02 3kdgA02 3keyA02 3kk7A03 3kluA01 3kp1A03 3ks3A00 3kt7A02
3ku3B00 3ku7B00 3kwlA04 3kyzA00 3l4gC01 3l4jA02 3l6iA00 3l7iA01 3l7iA02 3l8wA00
319aX01 31hoA01 31kmA02 31m1A02 31m1B01 31mmA01 31mmC03 31y7A01 3m1cA01 3m1cB01
3m7gA01 3m7kA00 3mb5A01 3me5A03 3mjfA04 3mm5B01 3mmhA00 3mmjB01 3mogA03 3mqzA00
3mt0A00 3mtvA02 3n01A00 3n28A02 3n4pC00 3n54B03 3n6rA03 3n6xA02 3n75A04 3n89A01
```

```
3n8bB00 3na2D00 3natA01 3nctB00 3ndhA00 3ne8A00 3nekA02 3nr5A00 3nuhB02 3nuhB03
3nycA02 3o2iA00 3o3mB02 3o3mD03 3o65E01 3o6qA02 3o8mA03 3od1A02 3od8F00 3oheA00
3okgA02 3ondA01 3onqA02 3oqgB00 3or1A02 3os4A00 3oxpA00 3oy2A01 3p0yA00 3p1yA01
3p3eA02 3p42D01 3pbtA02 3pdiA02 3pieC01 3pkzG00 3p18A02 3plwA00 3pr6A00 3psmA00
3pstA01 3pviA00 3pvzA02 3px4A03 3q1cA01 3q23A02 3q23A06 3q6bA01 3q8gA02 3qexA01
3qexA03 3qexA06 3qi7A03 3qvpA03 3qwuA03 3qx3A01 3r1xA02 3r1xB01 3r5dA01 3r5dA02
3r8jA00 3rgzA02 3rk1B02 3rl5A00 3rlfF02 3rnvA00 3rpeB00 3rrkA01 3rrkA03 3rsiB01
3rsnA00 3rtxA02 3rvcA00 3s1sA02 3s2rA01 3s83A00 3sbmA02 3sfvB01 3sj5A00 3sm4A00
3sqlB02 3ssoA01 3sxuA00 3sxuB00 3szyA02 3t3lA00 3t5tB01 3t7aA01 3tdgA01 3tdnA00
3tekA00 3tewA01 3tewA03 3thrA01 3tixB02 3tixB03 3tlaA02 3ttcA01 3ttcA02 3ttcA03
3tu3B01 3tutA01 3tvyA02 3tw8A01 3tw8A02 3u02A01 3u02A02 3u2aA00 3u52E01 3u5ek00
3u7qA02 3u97A00 3u9tA04 3uebF00 3uhmA01 3ungC01 3ushB00 3v3lB00 3v3tA02 3v46A00
3v4gA02 3v67A01 3v96A01 3vbcA00 3vcxA01 3vdpA02 3venA03 3vkwA01 3vmkA00 3vorA00
3vqtB03 3vrdB03 3vthA01 3vtiA03 3vtiA06 3vusA00 3vx8A01 3vx8A02 3vz9B00 3w0lB03
3w0oA01 3w1eA01 3w1eA02 3w1oA00 3w7tA04 3wa2X02 3wcnA01 3wcoA01 3wcqA00 3weeA03
3wh1A02 3wh3A00 3wnzA04 3wryA02 3wsfB01 3wx4A00 3wz2B00 3x01B01 3x01B02 3x34A00
3zihB00 3zqsA02 3zx4A02 3zyyX03 3zyyX04 4a2aA02 4a57A01 4a57A02 4a5zB00 4acfA01
4alzA01 4alzA03 4am6A03 4arcA05 4at0A02 4au1A00 4aukA01 4aukA02 4az3B00 4b1yB03
4bbyA02 4bbyA05 4bbyB04 4beuA02 4bgbB01 4bhqA00 4bi3A01 4bjjA00 4bjyA02 4bndA02
4bqnB01 4brcA02 4bs9A01 4bs9A04 4bs9A05 4bt2A02 4bvxB01 4c12A01 4c1bA02 4c1bB01
4c2mA09 4c97A02 4cgsB00 4chiB01 4ckbA01 4ckbA02 4cngA00 4cvnG00 4d3tA02 4d3tA03
4da2A02 4dczA00 4dduA04 4djbA00 4dkkA02 4dmgA02 4dx5A02 4dx5A04 4dx8J01 4dzoA02
4e3yA00 4e4rA01 4e4rA02 4e6nB00 4e6zA01 4ea9A01 4eadA03 4ebrA00 4egcB00 4ei7B01
4eo0A00 4ep4A00 4es1A00 4esjA01 4espA00 4esqA00 4eu0A02 4ew5B00 4eyyQ02 4f1vA02
4f3mA00 4fbwA02 4fcaA02 4fczA00 4fhdA01 4fhdA02 4fprB00 4fsdA02 4ftfA00 4fvmA02
4fvmA08 4fyyB01 4fzlA02 4g0aA01 4g0aB02 4g1iA02 4g1iB01 4g1qA04 4g1qB01 4g26A02
4g29A00 4g38A01 4g4sO01 4g6tA00 4g7nA02 4gj4B00 4g16A01 4gmuA01 4gmuA03 4gsxA03
4gvbA00 4gvqA01 4gvqA02 4gwbA00 4gywA03 4gywC04 4h4dA02 4h4dA03 4h61A00 4h63Q04
4h7wA00 4hcwA02 4hpmA00 4hscX01 4hvzA01 4hvzA02 4i43B04 4i4tB01 4i4tF01 4i5tB00
4i66A00 4i6yA02 4i8oA01 4i8oA02 4i9fA03 4ia6A02 4id9B02 4igiA00 4ihqA01 4ii2A01
4ii2A06 4iikA00 4iiwA01 4impA02 4ip2A02 4iqnC00 4ivvA00 4ix9D00 4ixjA01 4ixjA02
4j32A00 4j39A01 4j4hA01 4j7hA02 4j8lA02 4jb1A03 4jbdA02 4jc0A01 4jc0A02 4jc0A03
4je3B00 4jehA01 4jiuA00 4jk8B01 4jtmA00 4k05A01 4k05A02 4k8gA02 4kk7A01 4kmdA02
4krgA02 4ks9B02 4ksaA01 4kzsA03 4l4qA02 4l4qB01 4lf0A00 4llgM00 4lmyA02 4lttA00
4lviA01 4lvnP00 4lxqB00 4m02A01 4m0wA01 4m1xD00 4m5dA03 4m5dA05 4m8aA00 4mfkA02
4mh8A04 4mlvA03 4mncA00 4mnrA01 4muqA01 4n2pA00 4n3sA03 4n4nB00 4n7qA02 4n8nC00
4ndoB00 4ng0B00 4njcA00 4nkbA01 4nohA01 4nurA01 4nzrM01 4nzrM03 4o2hA00 4o4fA00
4o5qA01 4o6uA00 4o8sA01 4ofzA03 4oi3A00 4oltA02 4omfB02 4ouhC00 4p02B02 4p02B04
4p1mB01 4p3hA00 4pk9A00 4ps6A00 4pwqA01 4q28A00 4qbuA01 4qjvA03 4qmdA00 4r1qB01
4r7rA00 4r80A00 4rekA02 4reoA01 4reoA02 4rh8C00 4s39A01 4tpsA00 4tpsD00 4tpvA00
4u9hS01 4ua6A00 4udxX02 4ue8A00 4uhvA02 4uoiC00 4usaA03 4usaA04 4uuwB02 4uwhA02
4v0sB00 4w8hA00 4wfoA04 4wiqA02 4wk0B01 4wpyA01 4wx4A00 4x33A00 4x5wA01 4x9tA01
4xb6F00 4xduA00 4xjxA02 4xjxB01 4xlzA00 4xpmB00 4xqcA02 4xr8F01 4xwwA02 4xxfA00
4yaaA00 4yapA01 4ycbB00 4yorB00 4z3xA01 4zyaB00 4zyeA01 5a0yA01 5a0yA02 5a0yC00
```

 5a1iA03
 5a71A00
 5agrA00
 5an9F02
 5aoxE00
 5aunA01
 5aysC00
 5b3pA00
 5b66002

 5b6cA02
 5b7wA01
 5b7wA02
 5bw0F00
 5c17A00
 5c50B00
 5cdkA00
 5cgqB01
 5cphA00
 5cqgA02

 5cqgA04
 5d1pA01
 5dmhB01
 5dmhB02
 5dnyA02
 5dp2A01
 5e1A00
 5gjiA00
 5gmA02
 5grmA02

 5gs7A01
 5h3xA03
 5hb6B00
 5heeA00
 5hqtA01
 5hsqA03
 5hweA01
 5hweA02
 5gmA02
 5hweA03
 5hweA03</td